A STRATEGY TO MAKE SOLUBLE INTEGRAL MEMBRANE PROTEINS IN VIVO

by

Han-Sol Won

B.Sc., The University of British Columbia, 2013

A THESIS SUBMITTED IN PARTIAL FULFILLMENT OF

THE REQUIREMENTS FOR THE DEGREE OF

MASTER OF SCIENCE

in

THE FACULTY OF GRADUATE AND POSTDOCTORAL STUDIES

(Biochemistry and Molecular Biology)

THE UNIVERSITY OF BRITISH COLUMBIA

(Vancouver)

August 2016

Abstract

Membrane proteins play significant roles in fundamental biological processes, such as transport of molecules across the membrane, triggering intracellular signaling, maintenance of cell structure and utilization of energies. They are known to comprise about 30 % of genes of entire genome; they constitute around 60 % of current drug targets. Despite their importance, our knowledge about membrane proteins lags far behind that about the soluble proteins. This is chiefly because of their nature that hydrophobic domains of integral membrane proteins are embedded within the phospholipid bilayer and because of the fact that they are generally unstable following extraction from their native membrane environment by detergents. It is also true that available techniques for purifying, analyzing and handling membrane proteins are optimized for water-soluble proteins.

Hence, a strategy to solubilize membrane proteins in vivo in structurally relevant conformations by fusing membrane proteins with membrane scaffold protein (MSP) could be an alternative to detergent extraction and in vitro solubilization, allowing the direct expression of soluble membrane proteins in living cells. The MSP, which has an amphipathic helical domain, is thought to protect or shield the hydrophobic transmembrane domain of membrane proteins by sequestering them from aqueous environment.

To explore this strategy, an ATP binding cassette (ABC) transporter, MsbA, a known lipid flippase was initially chosen as a model protein. MsbA was fused to maltose binding protein (MBP) and MSP at its N-terminus to increase its expression level and to promote solubilization respectively. It was shown that MsbA fusion construct (MBP-MSP-MsbA) was produced in an

appreciable amount in water soluble form post detergent wash in the oligomerization state of a functional dimer and was able to hydrolyze ATP.

Preface

Design of the initial constructs, MSP1-MsbA and MSP3-MsbA was performed by Michael Carlson and John Young.

Design of the constructs, MBP-MSP1-MsbA and MBP-MSP3-MsbA that are investigated and presented in this thesis was done by me.

I conducted most of the experiments presented here. All the figures and tables were designed and created by me. Michael Carlson helped with lipid extraction experiment and analysis of the results, and the experiments introduced in Appendix C, analysis of MBP-MSP1-Stop codon were performed by Harpreet Sandhu.

Table of Contents

List of Tables

List of Figures

List of Abbreviations

ABC	ATP binding cassette
ATP	adenosine triphosphate
CL	cardiolipin
DDM	n-Dodecyl-β-D-maltopyranoside
DNA	deoxyribonucleic acid
DTT	dithiothreitol
E. coli	*Escherichia coli*
EDTA	ethylenediaminetetraacetic acid
ER	endoplasmic reticulum
IPTG	isopropyl-β-D-thiogalactopyranoside
kDa	kilodalton = 1000 grams/mole
LB	luria broth
MBP	maltose binding protein; MalE
MSP	membrane scaffold protein
NBD	nucleotide binding domain
Nd-MsbA	Nanodisc MsbA
PAGE	polyacrylamide gel electrophoresis
PCR	polymerase chain reaction
PDB	protein data bank
PE	phosphatidylethanolamine
PG	phosphatidylglycerol

PS	phosphatidylserine
pI	isoelectric point
PMSF	phenylmethylsulfonyl fluoride
SDS	sodium dodecyl sulfate
TEA	triethylamine
TLC	thin layer chromatography
TMD	transmembrane domain
Tx-100	triton x-100
Vi	vanadate

Acknowledgements

There are many people to thank. I would first like to thank my supervisor, Dr. Franck Duong, for providing me an opportunity to work in his lab and giving me this fascinating project to research. I really appreciate your generous guidance, supports and encouragement during the training in your lab. I would also like to thank my supervisory committee members, Dr. Roger Brownsey and Dr. Robert Molday, and my external examiner, Dr. Dieter Brömme for their input and valuable advice through the process of my research projects.

I would give lots of thanks to my brilliant past and current lab members of the Duong lab: Dr. Hai-Tuong Le, Dr. Badreddine Douzi, Dr. Huan Bao, Allan Mills, Michael Carlson, John Young, and Harpreet Sandhu, who have given me so much valuable advice and suggestions on many different aspects during my study.

I would like to acknowledge the University of British Columbia and Canadian Institutes of Health Research for financial support.

Lastly, I would like to appreciate my family and friends for their unconditional love and limitless support throughout the years of education. Without them, I would not be able to complete this thesis.

Dedicated to my family

Chapter 1: Introduction

Biological membranes are essential for cell integrity and compartmentalization, acting as an insulator and a selective filter between the cytoplasm and the outside medium, and between different intracellular compartments. It is mainly composed with a phospholipid bilayer and houses a number of particular proteins which are called membrane proteins that enable effective communication between cells or compartments and their environment.

Membrane proteins make up about one third of the entire human genome, representing approximately 20 to 30 % of the proteome (1). They play significant roles in fundamental biological processes, such as transport of molecules across membranes, triggering intracellular signaling, maintenance of cell structure, and extraction and utilization of chemical energy. Membrane proteins also represent more than 60 % of current drug targets (2). The largest family of drug targets among membrane proteins is G-protein-coupled receptors (GPCRs) – the malfunction of these receptors contributes to serious disorders such as hypertension, stroke, and cancer (2). The disruption of functions of other types of membrane proteins such as ion channels also triggers various diseases, including cystic fibrosis, Bartter syndrome and paralysis (2).

1.1 Current limitations of studying membrane proteins

Despite their significant representation within the genome and their essential roles in many biological processes, membrane proteins have been notoriously difficult to study because of their partially hydrophobic surfaces, flexibility, and lack of stability, which leads to challenges at all levels: from expression, solubilization, purification, to structural and functional studies (1).

In order to study membrane proteins, it is required to have special systems for in vitro work so that their high hydrophobicity can be satisfied. It is ideal to reconstitute them in the natural membrane environment in their native conformation after purification, which has led to development of several techniques. Membrane proteins have been reconstituted into micelles of detergent or liposomes. Although both techniques have their own advantages, they also have major drawbacks.

For instance, detergents are one of the most effective materials to solubilize membrane proteins, yet the choice of detergent requires diligent care and effort, since detergents can alter structures of membrane proteins, rendering them inactive, and can interfere with some downstream applications. Mild detergents are required to avoid denaturing the target membrane protein; nonionic or zwitterionic detergents are recommended over ionic detergents for stability of proteins while the opposite is true for solubilization efficiency (3). Detergent micelles usually lack a uniform structure and have non-ideal optical properties such as light scattering and absorbance (4). There is also high probability of aggregation of detergents besides membrane proteins, which can cause structural rearrangements not found in native membranes and the interference with some assay techniques (5). The fact that detergent micelles do not provide a lipid bilayer environment

for membrane proteins to properly function limits their use for functional studies on membrane proteins. A generic membrane protein in a detergent micelle is illustrated in Figure 1.1.

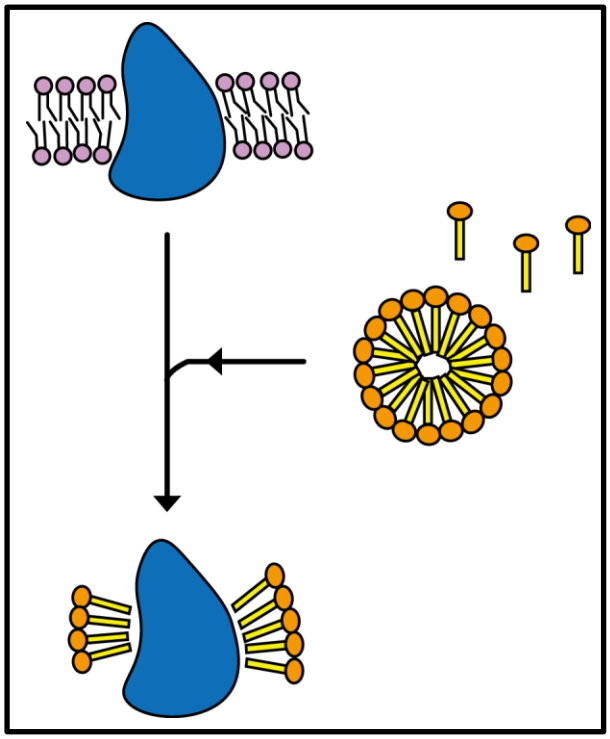

Figure 1.1 Schematic to illustrate detergent solubilization of a membrane protein
Membrane protein is shown in blue, initially embedded within the lipid bilayer (purple head group). Addition of detergent yields membrane protein incorporated into detergent micelle. Detergent micelle and monomers are depicted with orange hydrophilic head and yellow hydrophobic tail.

Another commonly used method to characterize membrane proteins is to reconstitute them using liposomes to produce a proteoliposome. A proteoliposome is composed of a liposome, a

spherical lipid bilayer that can range in diameter from 30 nm up to few micrometers with membrane protein incorporated in it (6). Proteoliposomes are generally formed according to one of two methods. The first method involves adding a protein-detergent mixture into a mixture of liposomes and detergent. Addition of protein to the liposomes is followed by a rapid dilution with buffer, which reduces the detergent concentration to below the critical micelle concentration (CMC). This causes the micelles to become destabilized, and thereby promotes incorporation of membrane proteins into the liposomes. An alternative method involves destabilizing liposomes with the addition of detergent, which disrupts the liposome bilayer, facilitating incorporation of proteins into the liposomes (8). A generic proteoliposome is depicted in Figure 1.2. A major advantage of proteoliposomes is that membrane proteins are incorporated within a lipid bilayer that enables compartmentalization of the membrane. However, the reconstitution process imposes constraints such as the orientation of the protein as well as the morphology and the size of the proteoliposomes (7). Although genuine efforts have been made to overcome many of these issues, methods for synthesizing proteoliposomes with precisely controlled size, stoichiometry and absolute directionality are yet to be fully optimized (4).

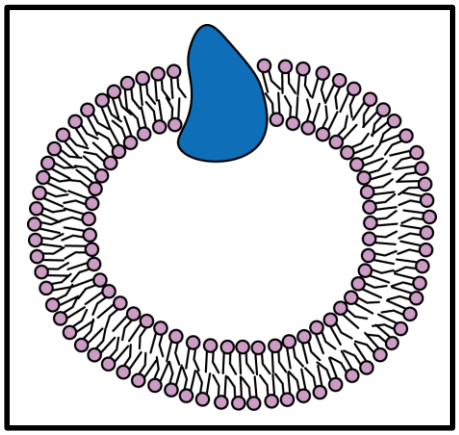

Figure 1.2 Proteoliposome
Proteoliposome is composed of a liposome in which a membrane protein is incorporated. Proteoliposomes enable compartmentalization of the membrane. Membrane protein is shown in blue and the hydrophilic head groups of the phospholipid in the lipid bilayer in lavender.

In addition to the detergent micelles and proteoliposome reconstitution, other approaches such as the use of tripod amphiphiles and amphipols have been described as additional methods to study membrane proteins. Tripod amphiphiles are composed of one head group, three hydrocarbon chains, and a branch point either within the hydrophobic portion or within both hydrophobic and hydrophilic portions (9). Amphipols are amphipathic polymers with a hydrophilic backbone and hydrophobic side chains that adsorb onto the transmembrane domain of membrane proteins (10).

1.2 Nanodisc

Nanodiscs (nanoscale discoidal) has been one of the most effective and widely used means of characterizing membrane proteins since its invention in 2002. Nanodiscs provide a native-like lipid environment for membrane proteins by providing a phospholipid bilayer surrounded by two membrane scaffold proteins (MSPs). MSPs are designed based upon modifications of the human serum apolipoprotein A-I in such a way that the N-terminal globular domain is deleted and the length of the remaining amphipathic alpha helical domain is adjusted to produce various sizes of MSPs (Figure 1.3). Genetic modifications have been performed by Sligar et al. to enhance monodispersity of nanodiscs and to ensure optimal expression in *E. coli* (11). The amphipathic nature of the MSP is a key to promote solubilization of membrane proteins. The hydrophobic face of MSP can shield hydrophobic fatty acyl chains of bilayer and hydrophobic transmembrane domains of a target protein while its hydrophilic surface can face an aqueous environment. The amphipathicity of MSP provides the highly soluble and stable nanodiscs containing an encapsulated membrane protein in the absence of detergents.

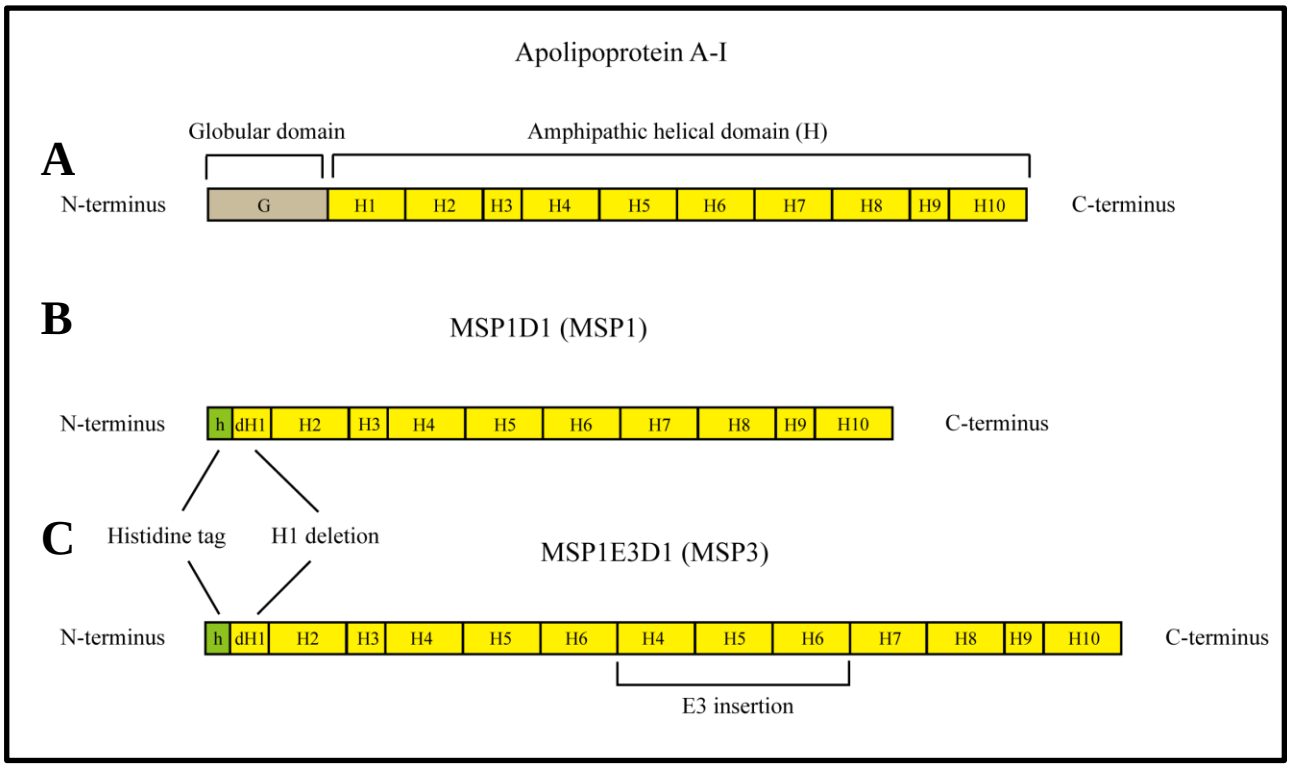

Figure 1.3 Schematic illustration of apolipoprotein and membrane scaffold proteins
Apolipoprotein and two commonly used membrane scaffold proteins (MSP1 and MSP3) are shown. A. Apolipoprotein A-I contains an N-terminal globular domain (G) and ten amphipathic helical domains (H). B. MSP1D1 consists of an N-terminal histidine tag (h) and ten amphipathic helical domains (H). C. MSP1E3D1 is the same as MSP1D1 except that it contains the E3 insertion in the middle. Yellow rectangles represent helices numbered from 1 to 10. dH1 represents H1 with its small portion being deleted in both MSP1 and MSP3.

The fact that the size of nanodiscs can be controlled by the length of the MSP and that phospholipid compositions can be modified has allowed flexibility to accommodate membrane proteins with many different topologies into nanodiscs, including single to multiple transmembrane segments, and multi-protein complexes (4, 12). Besides these advantages of the

control of size and lipid composition, nanodisc reconstitution provides additional merits such that the nanodisc reconstituted membrane proteins are produced in a homogeneous and monodisperse form, their oligomerization states can be controlled, and they have access to both sides of the membrane (13).

From extensive research aimed at understanding structural dynamics and functional properties of nanodiscs for the last 14 years, it has been demonstrated that nanodiscs are suitable and applicable to many different techniques. For example, nanodiscs can engage with many analytical techniques such as affinity chromatography, imaging technologies, and biosensor technologies (13). They can be adsorbed directly on surfaces or captured via tags incorporated in the MSPs, which makes them useful for deducing interactions with other partner proteins and kinetic studies through modified matrix-assisted laser desorption and ionization (MALDI) or surface plasmon resonance (SPR) (13). Furthermore, it has been shown that nanodiscs are suitable for structural studies of proteins using NMR spectrometry, small angle x-ray scattering technique (SAXS), atomic force microscopy (AFM) or electron microscopy (EM) (4).

1.2.1 Nanodisc reconstitution

In brief, nanodiscs are produced by mixing solutions of phospholipids, purified membrane scaffold proteins and detergent extracted membrane proteins. It is a self-assembly process which occurs upon removal of detergent by polystyrene biobeads (Figure 1.4).

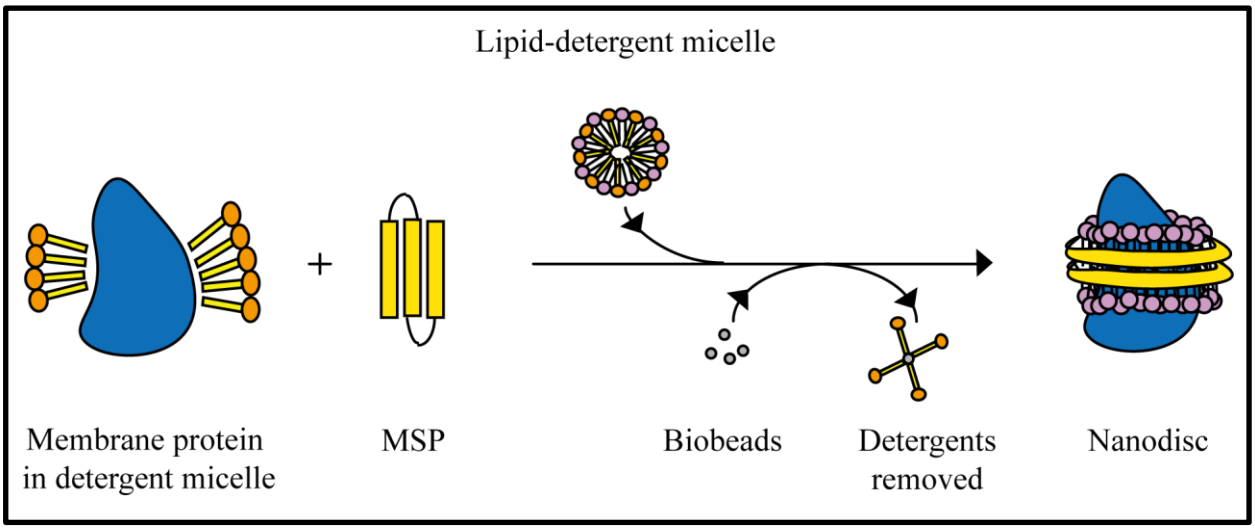

Figure 1.4 Schematic representation of nanodisc reconstitution
A membrane protein (blue) is extracted with detergent (orange head groups) and then incubated with membrane scaffold protein (MSP, yellow) and lipids (purple head groups) in the presence of detergent. The addition of biobeads facilitates the removal of detergents.

1.3 Membrane scaffold protein

The membrane scaffold protein is derived from human serum apolipoprotein A-I. Apolipoproteins are amphipathic and involved in transporting lipids in the blood (14). There are several different types of lipoproteins with distinctive morphologies, sizes, and functions (15). Among them, apolipoprotein A-I (ApoA-I) is the major protein component of high density lipoproteins (HDL) (16). There have been various studies to understand ApoA-I structure; it was shown that pre-mature HDL particles with low levels of cholesterol are discoidal in shape while mature HDL particles upon esterification of cholesterol by lecithin:cholesterol acyltransferase adopts a spherical shape with three ApoA-I molecules (17). Since MSP is derived from ApoA-I

and shares common features, understanding structural characteristics of HDL would help to understand structural dynamics of nanodisc assembly. Apolipoprotein A-I is composed of an N-terminal globular domain followed by ten amphipathic helices, including two 11-residue helices and eight 22-residue helices with glycine or proline residues at either end (18). The crystal structure of full-length ApoA-I shows that it contains an N-terminal four-helix bundle and two shorter C-terminal helices (Figure 1.5 A, PDB 2A01) (19). However, when the N-terminal globular domain is deleted, ApoA-I adopts a discoidal shape with four ApoA-I molecules (Figure 1.5 B, PDB 1AV1) (20). Although the high resolution structures of ApoA-I with lipids and ApoA-I in discoidal HDL particles have not been solved yet, the majority of the experimental data obtained so far supports the double-belt model of discoidal HDL structure (18). For nanodiscs, it has been demonstrated by small angle x-ray scattering and NMR spectroscopy that nanodiscs adopt a double-belt structure in which two copies of truncated ApoA-I encircle the lipid disc in an antiparallel manner, and they are rotated in such a way that the maximum number of intermolecular salt-bridges are satisfied. The general illustration of a nanodisc is shown in Figure 1.4 (21, 22). It was revealed from hydrogen exchange mass spectrometry that MSP in nanodiscs is dynamic and flexible even with a high percentage of helical content and its significant hydrophobic interactions with lipids (18).

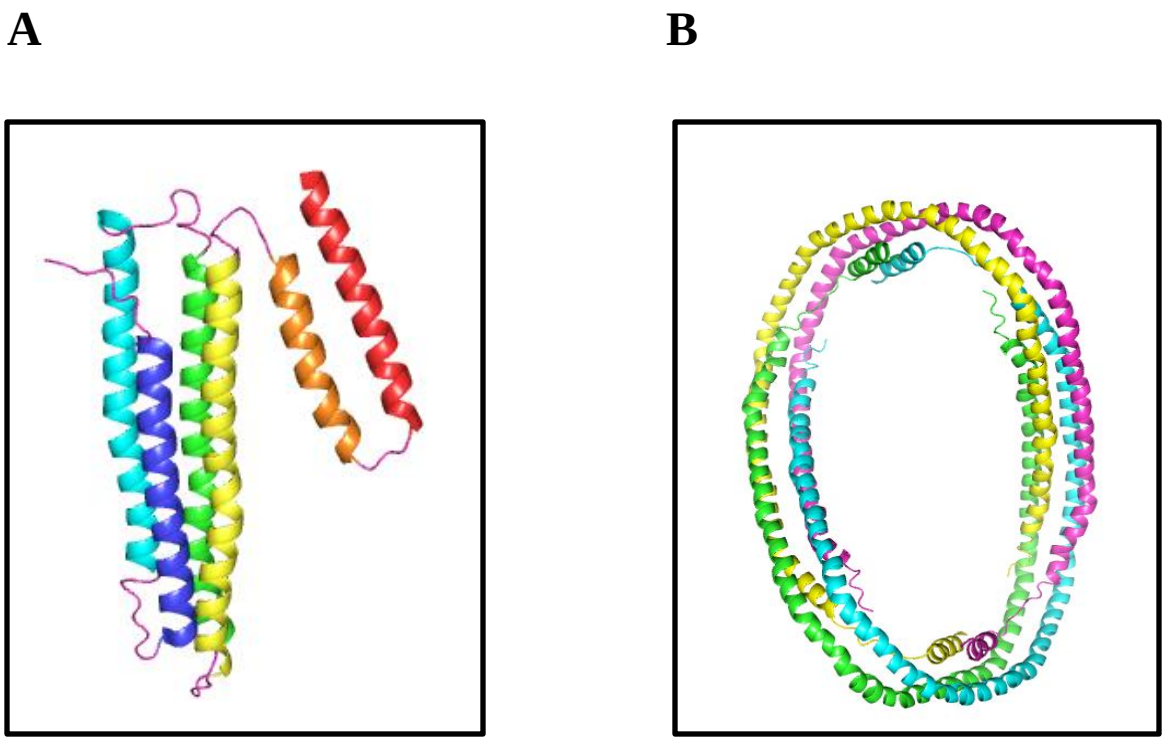

Figure 1.5 Crystal structures of apolipoprotein A-I
A. Crystal structure of full length apolipoprotein A-I without lipids at the resolution of 2.4 Å (PDB 2A01). The six helices in the structure are coloured blue, cyan, green, yellow, orange, and red. Loops are coloured purple. B. Crystal structure of ApoA-I with the N-terminal globular domain deleted (ApoA-I Δ(1-43)) without lipids at the resolution of 4 Å (PDB 1AV1). The structure shows a complex of four ApoA-I molecules coloured purple, yellow, cyan, and green.

1.4 ABC transporters

ATP binding cassette transporters are integral membrane proteins that constitute one of the largest families of membrane proteins (23). The family of ABC proteins mediates transport of a wide variety of compounds such as amino acids, drugs, sugars, ions, toxins and lipids across cellular membranes, and are conserved from bacteria to human (24). They acquire the energy for

mechanical work to transport their substrate from ATP binding and hydrolysis. The translocation of substrate requires binding on one side of the membrane and release on the opposite side and is coordinated by ATP binding and hydrolysis, and release of ADP and Pi. ABC transporters are also known to be involved in multidrug resistance (25). All ABC transporters share the same core modular architecture: two transmembrane domains (TMDs) and two nucleotide binding domains (NBDs). In general, TMDs are embedded within the membrane bilayer and form a transport pathway by mediating accessibility to either side of the membrane, while the NBDs are involved in ATP binding and hydrolysis. Since each transporter is designed to recognize and translocate its own specific substrate, TMDs of transporter are diverse in sequence and vary in total number of membrane spanning helices. On the other hand, NBDs are highly conserved among ABC transporters. NBDs contain Walker A and B motifs for ATP binding, and an ABC signature sequence, LSGGQ (26, 27). Other highly conserved motifs such as the D-loop, Q-loop and H-loop are crucial for ATP hydrolysis and inter-domain communication (28, 29). Intensive structural studies of ABC transporters and isolated NBDs have suggested that they are structured in twofold or pseudo-twofold symmetry between monomers (30-42).

1.5 MsbA

The membrane protein, MsbA is an ABC transporter found in Gram-negative bacteria. MsbA shares significant sequence homology with human multidrug resistance protein 1 (MDR 1) and LmrA from *Lactococcus lactis*, both of which are drug efflux pumps causing multidrug resistance (MDR) (43). The gene for MsbA encodes a 64.5 kDa half-transporter, comprised of a TMD with 6 membrane spanning helices and a NBD (44-47). It is presumed to function as a homodimer (51). A number of x-ray crystal structures of MsbA from several bacterial species have

been solved (48: PDB 3B5W, 3B5X, 3B5Y, 3B5Z, 3B60); stereoviews of 3 conformations of MsbA generated by Ward et al. (48) are represented in Figure 1.6. Several lines of evidence have suggested a role of MsbA in translocation of lipid A and other phospholipids from the inner to the outer leaflet of the cytoplasmic membrane (44, 45, 49, 50). MsbA is an essential protein in *E. coli*; it was demonstrated that loss of function mutation results in rapid cessation of cell growth with accumulation of lipid A and phospholipids in the inner membrane, and subsequent formation of inner membrane invaginations (44, 46). Eckford et al. recently demonstrated that the ATPase activity of MsbA was stimulated up to 2 fold by a mixture of *E.coli* lipids which contains phosphatidylethanolamine (PE), phosphatidylglycerol (PG), phosphatidylserine (PS), and smaller amounts of other species like lipid A (49). It was also shown that its ATPase activity was modulated by amphipathic drugs that are substrates for LmrA and MDR 1 (49). There is evidence in the literature that the binding sites of MsbA for the amphipathic drugs and lipid A are distinct from each other (51). Furthermore, just like other ABC transporters, ATPase activity of MsbA was inhibited in the presence of vanadate (Vi) (49). The fluorescence lipid flippase assay conducted by Eckford et al. (49) demonstrated the ATP-dependent translocation of lipids by MsbA for the first time; MsbA reconstituted into proteoliposomes of *E. coli* lipid exhibited flippase activity for both head group- and acyl chain-labelled derivatives of PE and PS as well as chain-labelled PG, and sphingomyelin (SM) (50). The highest flippase activity of MsbA was observed with PE (50).

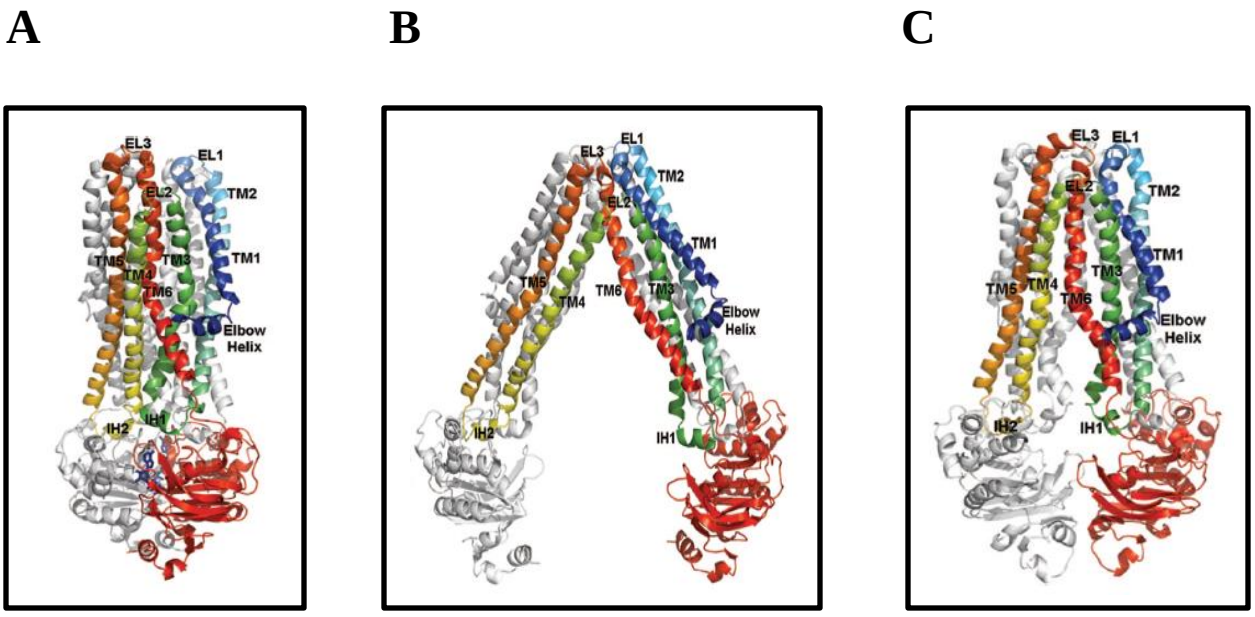

Figure 1.6 Illustration of 3 conformations of MsbA
Crystal structures of MsbA from various species including *E.coli* were solved by Ward et al. (PDB 3B5W, 3B5X, 3B5Y, 3B5Z, 3B60). Illustration of 3 conformations of MsbA: A. With the nucleotide, AMPPNP bound, B. Open-apo, and C. Closed-apo. All these representations are adapted from Ward et al. (2007). One monomer is shown by rainbow colors (N-terminus in blue, and C-terminus in red), and the other monomer is shown in grey. Transmembrane helices (TM1-6), extracellular loops (EL1-3), and intracellular helices (IH1-2) are labeled accordingly.

1.6 Thesis investigation

Despite strenuous efforts to develop and improve various tools to study membrane proteins, there are still many shortcomings in the methods available, requiring more sophisticated and advanced techniques to be established.

In this thesis, a strategy that might be used as an alternative method to solubilize membrane proteins is introduced. The basic idea of the strategy is to synthesize a soluble membrane protein

by fusing it to MSP, which is thought to protect or shield the hydrophobic domain of membrane proteins by sequestering them from aqueous environment at the beginning of its expression pathway in living cells. The major difference of the strategy investigated in the thesis from any of the techniques so far available is that it promotes solubilization of membrane proteins in vivo. Taking advantage of the crucial role of amphipathic MSP in nanodisc reconstitution, it is anticipated that the strategy can enable in vivo solubilization of membrane proteins in structurally relevant conformations and functionally competent forms by attached MSP. If successful, this strategy should provide an alternative to detergent extraction and in vitro solubilization, allowing the direct expression of soluble membrane proteins in living cells. In turn, it is hoped that this approach will promote relatively easy handling of membrane proteins to study their structures and functions, as well as providing a new means to study challenging insoluble and unstable membrane proteins that are otherwise hard to handle.

To examine the strategy, MsbA was initially chosen as a model protein for several reasons. Firstly, it is known to be well expressed from previous studies. A well expressed protein was chosen, so that, if the strategy failed, expression problems associated with the model protein could be ruled out as a reason for failure. It was expected that the MsbA fusion construct would be produced in large amounts in a water soluble form. Secondly, the gene for MsbA encodes a half transporter which must form a homodimer to be functional. Therefore, we anticipated that we would be able to assess whether the fusion construct was in its functionally relevant dimeric state by measuring its ability to hydrolyze ATP.

The gene for MsbA was genetically fused to MSP at its N-terminus to be soluble, and also fused with the maltose binding protein (MBP) to increase its expression level. The construct of the

fusion protein (MBP-MSP-MsbA) is illustrated in Figure 1.7. The fusion construct was purified by an amylose column using MBP as a tag and the purified fusion protein has been subjected to further analysis of its structure and function.

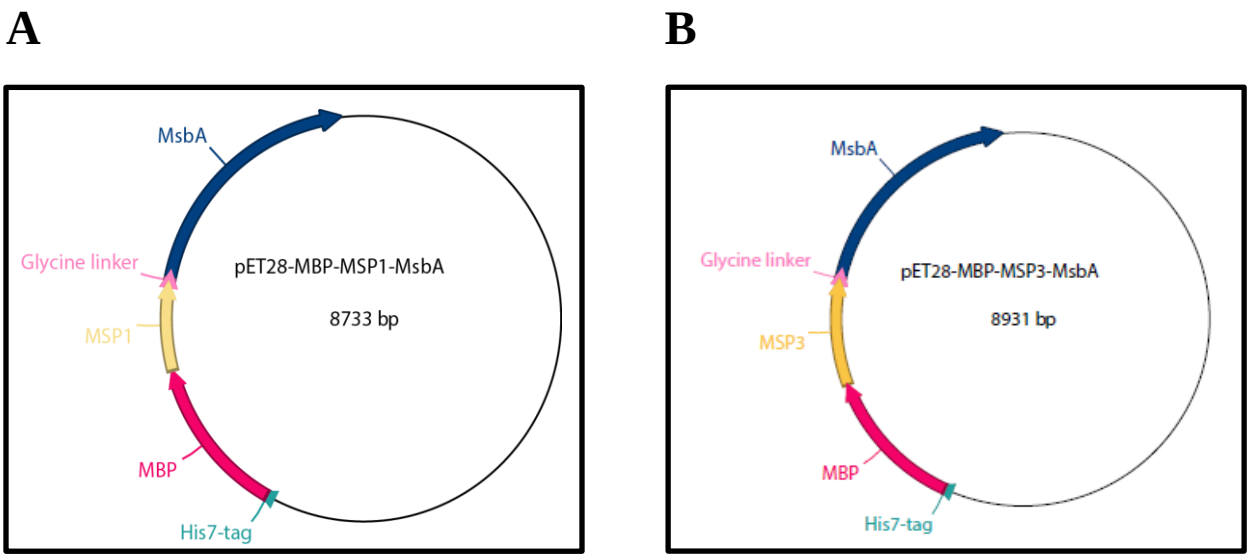

Figure 1.7 Illustration of the MsbA fusion constructs
A. The design of the fusion construct, MBP-MSP1-MsbA. B. The design of the fusion construct, MBP-MSP3-MsbA. Each component of the constructs is colour-coded with label and an arrow indicates the directionality of the constructs.

Chapter 2: Materials and methods

2.1 Membrane protein, MsbA

2.1.1 Materials

A plasmid, pET28-His_7-MsbA was already available in the laboratory. Salts and solvents were purchased from Fisher Scientific (Hampton, NH). The following materials were obtained as indicated: all antibiotics and isopropyl β-D-1-thiogalactopyranoside – Gold Biotechnology (St. Louis, MO); n-Dodecyl β-D-maltoside – Affymetrix (Santa Clara, CA); phenylmethylsulfonyl fluoride and Triton X-100 – BioShop (Burlington, ON); detergent adsorbent BioBeads® – Bio-Rad (Hercules, CA); purification columns and beads – GE Healthcare (Pittsburgh, PA); malachite green – Sigma-Aldrich (St. Louis, MO).

2.1.2 *E. coli* C43 (DE3) competent cells

Bacterial cells were streaked out on LB agar plate without antibiotics. A single colony was selected and grown overnight in LB media. Two batches of 125 ml fresh LB media containing 20 mM $MgSO_4$ were inoculated with 1.25 ml of preculture and incubated at 37 ˚C shaker until they reach $O.D._{600nm}$ 0.4 – 0.6. The cells were then centrifuged in 2 separate sterile falcon tubes at 4,000 rpm for 10 min at 4 ˚C. The pellets were gently suspended in 15 ml of TFB1 buffer (30 mM Acetate potassium, 100 mM KCl, 10 mM $CaCl_2$, 50 mM $MnCl_2$ and 15 % w/v glycerol; filtered), combined in one sterile falcon tube, and stored in ice for 10 min. The whole cells were centrifuged at 4,000 rpm for 10 min at 4 ˚C, and resuspended in 5 ml of TFB2 buffer (10 mM MOPS, 75 mM CaCl2,

10 mM KCl and 15 % w/v glycerol; filtered). Resuspended cells were stored in the ice for 30 min, and aliquoted as 50 – 100 µl into sterile 1.5 ml Eppendorf tubes.

2.1.3 Transformation of *E. coli* C43 (DE3)

One hundred microliters of *E. coli* competent cell (C43DE3) were incubated with approximately 50 ng of DNA at 4 ˚C for 30 minutes. The competent cell mixture was heat shocked at 42 ˚C for 45 seconds and chilled in the ice for 2 min. One milliliter of Luria Broth media was added and the mixture was vigorously shaken at 37 ˚C incubator for an hour. After the incubation, the whole mixture was centrifuged at 4,000 rpm for 1 min. Most of supernatant was discarded and cell pellet was suspended in residual supernatant which was spread onto the plate containing 50 µg/ml kanamycin. The plate was incubated at 37 ˚C overnight.

2.1.4 Expression of membrane protein, MsbA

Cells were grown overnight at 37 ˚C in 40 ml of LB media supplemented with 50 µg/ml kanamycin. Next day, the cultures were inoculated into 4 L of LB media in the presence of 50 µg/ml kanamycin and subjected to agitation at 37 ˚C. The cultures were induced with a final concentration of 0.5 mM IPTG at $O.D._{600nm}$ ~0.5, and allowed to grow for three more hours at 37 ˚C before harvesting.

2.1.5 Membrane protein extraction

Four liters of grown cells were harvested by centrifugation at 5,000 rpm (Beckman JLA 10.5 rotor) for 10 min, the cell pellet was suspended in 50 ml of buffer A (50 mM Tris-HCl pH 7.9, 100 mM NaCl and 10 % v/v glycerol), and a final concentration of 1 mM of phenylmethylsulfonyl fluoride was added before lysis. The cells were passed through a microfluidizer (Microfluidics Corp.) three times at 12,000 psi. The lysate was centrifuged at 6,000

rpm (Beckman JA 25.5 rotor) for 10 min to remove unbroken cells, cell debris and large inclusion bodies. Then, the supernatant was ultracentrifuged for 45 min at 55,000 rpm (Beckman Type 60 Ti rotor) at 4 ˚C. The pellet containing membrane proteins was resuspended in buffer A and solubilized with 1 % v/v n-Dodecyl β-D-maltoside overnight at 4 ˚C which was then spun again next day at 55,000 rpm for 45 min at 4 ˚C. The supernatant was collected for purification.

2.1.6 Purification of MsbA

A 5ml column pre-packed with Ni^{2+} sepharose high performance beads was used to purify His_7-tagged MsbA. The Ni^{2+} column was equilibrated in buffer B (50 mM Tris-HCl pH 7.9, 100 mM NaCl, 10 % v/v glycerol and 0.01 % DDM). The solubilized membrane fraction containing MsbA was loaded onto the column at a flow rate of 1 ml/min. MsbA was washed with buffer B supplemented with 30 mM imidazole and eluted with buffer B with 500 mM imidazole. Flow through and eluate were analyzed by SDS-PAGE, and elution fractions containing pure MsbA were pooled.

2.1.7 SDS-PAGE

10 %, 12 % or 15 % sodium dodecyl sulfate polyacrylamide gels were used to separate proteins. Five microliters of sample buffer (150 mM Tris-HCl pH 6.8, 10 % v/v glycerol, 2 % SDS and 1.25 % bromophenol blue) were mixed with each sample, and SDS gel was run at 45 mA for 50 min. A gel was soaked in Coomassie stain solution (40 % v/v methanol, 10 % v/v acetic acid and 0.25 % w/v Coomassie Brilliant Blue R-250), and destained in destain solution (20 % v/v ethanol and 10 % v/v acetic acid).

2.1.8 Nanodisc reconstitution

To make nanodiscs, purified membrane protein, lipids and membrane scaffold protein (MSP) are mixed together in a certain molar ratio which can be different for each membrane protein. For Nanodisc MsbA (Nd-MsbA) reconstitution, 1 nmol of MsbA was incubated with 4 nmol of MSP in TSGD buffer (50 mM Tris-HCl pH 7.9, 100 mM NaCl, 10 % v/v glycerol and 0.1 % w/v DDM) in total volume of 300 µl per a tube of reconstitution. No lipids were added during Nd-MsbA reconstitution. One hundred microliters of biobeads were added per a tube of mixture, which was then gently rocked at 4 ˚C for 16 h to adsorb detergent. The biobeads were removed by low speed centrifugation and Nd-MsbA was concentrated using a 4 ml Amicon Ultra-4 Centrifugal Filter (Millipore) with molecular size cut-off of 30 kDa.

2.1.9 Size exclusion chromatography

To remove any aggregates and free excess MSPs, the concentrated Nd-MsbA was subjected to size exclusion chromatography using a Superdex^{TM} 200 HR 10/300 column (Amersham) equilibrated with buffer A. Each of 1 mL fractions was collected and analyzed by both native-PAGE and SDS-PAGE.

2.1.10 Clear-native and blue-native PAGE

A non-denaturing gel with 4-12 % linear polyacrylamide gradient was prepared in native running buffer (25 mM Tris and 190 mM glycine pH 8.8). A clear-native PAGE was run in native running buffer while a blue-native PAGE was run in native running buffer at the anode and Blue G buffer (native running buffer plus 0.02 % w/v Serva Blue G Dye) at cathode. A clear native gel was stained and destained as described in section 2.1.7, and a blue native gel was destained only.

2.1.11 ATPase assay

ATPase activity was determined by monitoring release of inorganic phosphate using photo-colorimetric method. In the ice, 2 mM of ATP was added to ATPase assay buffer (50 mM Tris-HCl pH 7.9, 100 mM NaCl, 10 % v/v glycerol and 1 mM DTT) containing 1-5 μg of protein. ATP hydrolysis was initiated as the reaction mixture was placed at 37 ˚C at time 0 min. An aliquot of 20 μl of the reaction mixture was then taken out at each time point and mixed with 500 μl of malachite green molybdate solution. Malachite green molybdate forms a complex with free orthophosphate under acidic conditions and the formation of this green molybdophosphoric acid complex is detected at 660 nm on a Genesys^{TM} 10 uv spectrophotometers (Thermo Scientific). For ATPase inhibition assay, 2 mM vanadate (Vi) was added to the reaction mixture.

2.2 MsbA fusion constructs

2.2.1 Materials

All enzymes used in molecular cloning steps and amylose resin were purchased from New England Biolabs Inc. (Ipswitch, MA). The following materials were acquired as stated: primer oligonucleotides – Invitrogen (Carlsbad, CA); primary antibody for western blot – ABM Inc. (Richmond, BC); secondary antibody for western blot – LI-COR (Lincoln, NE); nitrocellulose membrane for western blot – Bio-Rad (Hercules, CA); thin layer chromatography plate – Millipore (Billerica, MA). Rest of materials were obtained as indicated in section 2.1.1

2.2.2 Polymerase incomplete primer extension (PIPE) cloning

Plasmids, pET28-His_7-MsbA, pET28-His_6-MSP1, pET28-His_6-MSP3 and pBAD33-maltose binding protein (MBP) were already available in the laboratory. Cloning was performed to produce the MsbA fusion constructs, pET28-His_7-MBP-MSP1-MsbA and pET28-His_7-MBP-MSP3-MsbA over two rounds of PCR; the first round PCR was done to insert MSP in front of MsbA and the second round PCR was completed to insert MBP at the very N-terminus of the fusion construct. The primers used for each PCR are listed in appendix A.

2.2.2.1 PIPE – polymerase chain reaction condition

Both inserts (MSP1 or 3 for first round and MBP for second round) and the vector plasmids (pET28-His_7-MsbA for first round and pET28-His_7-MSP1 or 3-MsbA for second round) were amplified by PIPE – PCR using approximately 0.5 µg DNA template, 10 pmol of primers, 200 µM dNTPs and 1 U of Phusion^{TM} DNA polymerase in recommended buffer to a final volume of 50 µl in a 0.2 ml thin wall PCR tube (Axygen) with an Eppendorf Mastercycler 5332 thermomulticycler under the condition listed below.

Table 2.1 PIPE – Polymerase chain reaction program

Step	Temperature	Time
1	95 ˚C	3 min
2	95 ˚C	30 seconds
3	$T_{anneal} = (T_m – 5$ ˚C)	30 seconds
4	72 ˚C	Elongation time depends on the length of the product (1 kb/min)
5	Go to step 2	Repeat 25 – 30 times
6	16 ˚C	Hold

2.2.3 Amplified DNA on agarose gel and DpnI digestion

A small amount of amplified PCR products was analyzed on a 1.0 % agarose gel in TBE buffer (89 mM Tris-HCl pH 7.9, 89 mM Borate and 2 mM EDTA) to ensure their amplification and subjected to DpnI digestion in 1X CutSmart® buffer (50 mM Potassium Acetate, 20 mM Tris-acetate, 10 mM Magnesium Acetate and 100 µg/ml BSA at pH 7.9) for 2 h at 37 ˚C. Then, digested vector PCR product and insert PCR product were mixed in 1:2 ratio respectively, and co-transformed into DH5α competent cell which was allowed to grow on LB agar plate supplemented with 50 µg/ml kanamycin. The correct placement of inserts into the vector plasmids was confirmed by sequencing at Genewiz Inc.

2.2.4 Expression of MsbA fusion constructs

Plasmid pET28 encoding N-terminal His_7 tagged fusion construct was transformed into *E. coli* strain C43 (DE3), was grown overnight for 14 h at 37 ˚C in 5 ml of LB media with 50 µg/ml of kanamycin. The culture was diluted into 500 ml of fresh LB media supplemented with 50 µg/ml kanamycin, and vigorously agitated at 37 ˚C until $O.D._{600nm}$ reached 0.5. A final concentration of 100 µM IPTG was added to induce cell, and it was grown for three more hours before harvested by centrifugation at 5,000 rpm (Beckman JLA 10.5 rotor) for 10 min. The cell pellet was suspended in 4 ml of buffer A (50 mM Tris-HCl pH 7.9, 100 mM NaCl and 10 % v/v glycerol), and a final concentration of 1 mM of phenylmethylsulfonyl fluoride was added before lysis. The cells were passed through a mini French Pressure cell press three times at 12,000 psi. The lysate was centrifuged at 6,000 rpm (Beckman JA 25.5 rotor) for 10 min to remove unbroken cells, cell debris and large inclusion bodies. Then, the supernatant was ultracentrifuged for 20 min at 70,000 rpm (Beckman TLA-110 rotor) at 4 ˚C. The supernatant containing soluble fraction was stored at - 80

˚C, and the pellet containing insoluble fraction was resuspended in buffer A and solubilized with 0.5 % Tx-100 overnight at 4 ˚C. The solubilized material was spun next day at 70,000 rpm for 20 min at 4 ˚C and the supernatant was stored at - 80 ˚C for further analysis.

2.2.5 Expression and localization test

To test if the fusion construct was expressed, 1 ml of cell culture was taken at each time point: before and after 1, 2, and 3 h of induction while growing. Each of 1 ml of whole cell aliquot was low spun by a table top centrifuge (Eppendorf) at 3,000 rpm, and cell pellet was suspended and lysed in 100 µl of 2 % SDS solution. Then, it was incubated at 42 ˚C for 10 min to shear DNA and reduce viscosity, and centrifuged at 13,200 rpm for 10 min. Supernatant was loaded onto SDS-PAGE.

To test whether the fusion protein was expressed as a soluble protein, small fractions at each step of low and high spin after cell lysis were analyzed on SDS-PAGE. After cell lysis and low spin, inclusion bodies/cell debris were resuspended in buffer A and loaded onto SDS-PAGE. After high spin, both cytosolic soluble proteins and insoluble membrane proteins were loaded onto SDS-PAGE. The insoluble membrane proteins were solubilized by Tx-100 overnight and high spun next day. Supernatant containing solubilized proteins was analyzed by SDS-PAGE.

2.2.6 Western blot

SDS gel was soaked into 1x transfer buffer (48 mM Tris, 39 mM glycine, 20 % methanol and 0.04 % SDS) and assembled to a transfer sandwich of papers/gel/membrane/papers wetted in transfer buffer. Proteins were transferred from the gel to nitrocellulose membrane for 50 min at 400 V with blot on the cathode and the gel on the anode. After transfer, the membrane was incubated with blocking buffer (5 % w/v non-fat milk solution) for 20 min at room temperature

and washed three times for 5 min each with TBST buffer (20 mM Tris-HCl pH 7.5, 137 mM NaCl and 0.05 % Tween-20). The washed membrane was incubated with anti-His primary antibody in 3 ml TBST buffer (1:2000 dilution) for 45 min with gentle rotation at room temperature. The membrane was washed three times for 5 min each with TBST buffer, and incubation process was repeated with anti-Mouse secondary antibody (1:2000 dilution) in 3 ml TBST buffer for 45 min followed by three times wash step. The target protein on the membrane was then detected by Odyssey® fluorescence imaging system (LI-COR).

2.2.7 Amylose purification

2.2.7.1 Soluble fraction purification

A supernatant containing soluble fraction was loaded onto 2 ml amylose column equilibrated with loading buffer (20 mM Tris-HCl pH 7.9, 200 mM NaCl, 10 % v/v glycerol, 1 mM DTT, 1 mM EDTA and 0.05 % Tx-100), and flow through was collected. The column was washed in loading buffer to remove any non-specifically bound proteins, and the fusion protein was eluted with elution buffer (loading buffer plus 20 mM maltose). The flow through, wash and eluate were analyzed by SDS-PAGE.

The eluted fractions containing fusion construct were pooled and subjected to further purification by size exclusion chromatography. The pooled amylose fractions were injected onto a Superdex^{TM} 200 HR 10/300 column (Amersham) equilibrated with buffer C (20 mM Tris-HCl pH 7.9, 200 mM NaCl, 10 % v/v glycerol and 1 mM DTT). Fractions were collected and analyzed by both SDS-PAGE and 4-12 % native-PAGE. The pure soluble fusion construct was pooled and stored at - 80 ˚C for future use.

For sample preparation for thin layer chromatography (TLC) experiment later, the fusion protein from the soluble fraction was purified in the absence of detergent. All the buffers used in the amylose column purification contain no detergent. The rest of the purification steps are the same as described above.

2.2.7.2 Insoluble fraction purification

A Tx-100 solubilized insoluble fraction was diluted 10 times in loading buffer without Tx-100 to reduce the final concentration of Tx-100 to 0.05 %. Purification was processed as previously described in section 2.2.7.1.

2.2.8 Thin layer chromatography

To make radiolabeled lipids to use them as an internal standard for lipid extraction, 50 ml of *E. coli* BL 21 cells were grown in the presence of 1 μCi of radioactive ATP (γ-^{32}P). The cells were grown until stationary phase and spun down at 3,000 rpm for 10 min. The cell pellet was suspended in 1 ml of buffer A, which was frozen and stored in LEAD lined capsule at - 20 ˚C.

All protein samples to be analyzed were diluted to the same concentration prior to the lipid extraction. Five microliters of the radioactive cells were added to 300 μl of each protein sample to be analyzed at the very initial step of lipid extraction process so that it can act as an internal standard to track the total loss of lipid during the lipid extraction process and lipid spotting step on TLC plate. The rest of the steps were as followed. Three hundred microliters of chloroform and 600 μl of methanol were added to 300 μl of protein sample containing the internal standard, and the mixture was let sit for 30 min at room temperature after vigorous vortexing. Three hundred microliters of chloroform and 300 μl of water were added again, and the whole mixture was spun down at 3,000 rpm for 10 min. The upper liquid phase was discarded and the lower (chloroform)

phase was transferred into a new glass vial. The solvent was evaporated completely in a stream of nitrogen and the concentrated lipid was dissolved in 20 μl of chloroform.

The extracted lipid from each sample was then dotted 10 times by a capillary tube on TLC plate which was developed in the TLC developing buffer (chloroform:ethanol:water:TEA in 35:26:4:35 v/v ratios). The standard lipid sample consisting of PE, PG and CL was dotted besides the samples for reference.

The developed TLC plate was then dried till most of TEA was evaporated and lightly dapped with a charring reagent (10 % w/v $CuSO_4$ and 10 % v/v phosphoric acid). The TLC plate was dried over and heated for about 5 min at the heating block until spots became apparent.

The radiolabeled internal standard on the TLC plate was visualized by phosphor-imaging system after an overnight exposure (STORM PhosphorImager).

The intensity of those spots on TLC plate was determined by densitometry analysis by Image J, normalized and graphed for comparison of the amounts of lipids in each sample.

Chapter 3: Results

3.1 Nanodisc reconstitution of MsbA and its ATPase activity

3.1.1 IMAC purification of MsbA

The N-terminus 7-histidine tagged MsbA was over-expressed in C43 cells, and purified as described in section 2.1.6. The expression of MsbA was visualized on SDS-PAGE and was apparent after 3 hours of induction with 1 mM IPTG (Figure 3.1 A). MsbA elution fractions from Ni-NTA chromatography were analyzed by SDS-PAGE with Coomassie stain (Figure 3.1 B). Purification of MsbA expressed in C43 cells yields significant amount of pure MsbA in monomeric form as indicated by the predominant band in each fraction at the size of 65 kDa in Figure 3.1 B. A typical preparation yielded ~5.25 mg of purified MsbA from 4 L of cell cultures.

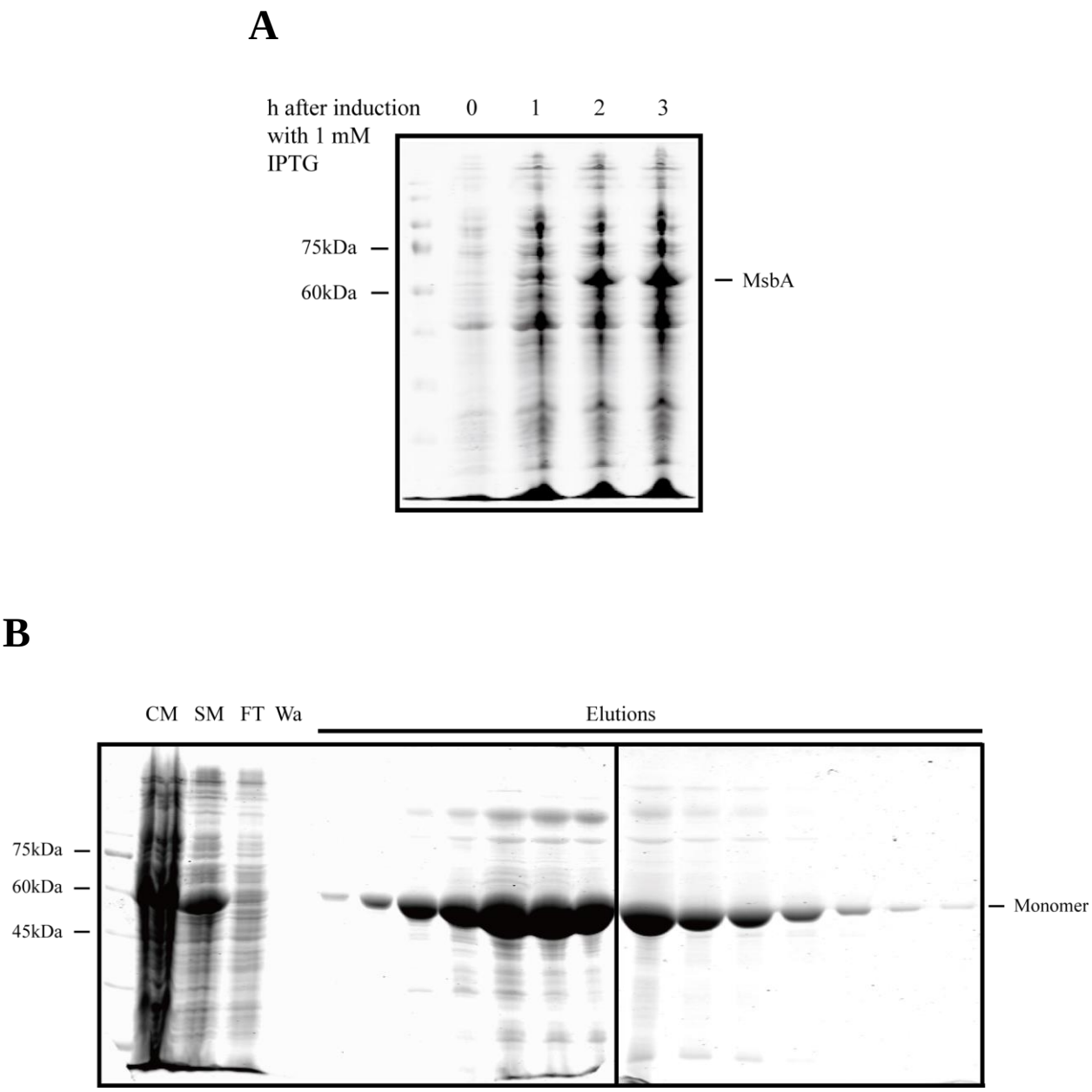

Figure 3.1 Expression and purification of MsbA

A. Expression of MsbA after 1, 2, and 3 hours of induction with IPTG was visualized on Coomassie stained SDS-PAGE. B. Ni-NTA purification of MsbA was performed as described in section 2.1.6. The solubilized membrane fraction containing MsbA was loaded onto Ni-NTA column equilibrated in buffer B, washed with 30 mM imidazole and eluted with 500 mM imidazole. Fourteen fractions each with 1 mL were collected and analyzed on SDS-PAGE. Abbreviations on

the gel: CM (solubilized membrane fraction), SM (diluted starting material), FT (flow through), Wa (wash).

3.1.2 Nanodisc reconstitution of MsbA

The purified MsbA protein was reconstituted into nanodiscs without any addition of *E. coli* lipids using a membrane scaffold protein (MSP). Both MSP1 and MSP3 were used to incorporate MsbA into nanodiscs. The amounts of MsbA and MSP were optimized to reduce the amount of free MSP and aggregates as much as possible before reconstituting in a large volume. Although the ratios of reconstitution were optimized, it was necessary to have a highly pure Nd-MsbA for future analysis to measure its ATPase activity. Hence, both MsbA nanodiscs with either MSP1 or MSP3 were purified by gel filtration to separate Nd-MsbA from aggregates and unincorporated MSPs. For Nd-MsbA with MSP1, the largest peak corresponding to an incorporation of MsbA with MSP1 was followed by a second peak corresponding to free MSPs (Figure 3.2 A). A small peak in the void volume (~8ml) eluting before the largest peak represents aggregates (Figure 3.2 A). For Nd-MsbA with MSP3, the gel filtration profile was similar to that of Nd-MsbA with MSP1; the largest peak corresponding to MsbA associated with MSP3 (Figure 3.2 B). There was less free MSP3 or large aggregates when analyzing Nd-MsbA with MSP3 than Nd-MsbA with MSP1.

The gel filtration fractions containing pure Nd-MsbA with MSP1 or MSP3 were analyzed on both clear and blue native gels. On a colorless native gel, the purified MsbA protein from a Ni-NTA column did not migrate into the gel but instead appeared as a smear on the top of the gel. It is generally found that membrane proteins migrate poorly through CN-PAGE because detergents that are associated with the membrane proteins are rapidly diluted during migration in the gel, causing the formation of protein aggregates. Another possible reason for retarded migration of the

purified MsbA is its high isoelectric point of 8.62 (Figure 3.2 C, lane 1). It is known that the migration of proteins on clear-native PAGE is also affected by the intrinsic charge of the protein such that only acidic proteins with pI < 7 migrate towards the anode (52). When MsbA was associated with MSP, its hydrophobic transmembrane domain was shielded from aqueous solution as the hydrophobic surface of MSP sealed around it. Nd-MsbA solubilized by association with MSP was thus able to migrate into the clear native gel and appeared as a distinct band as shown in lane 4 to 7 on clear native gels that show the fractions of each largest peak of gel filtration profiles for both Nd-MsbA with MSP1 and MSP3 (Figure 3.2 C and D). On a blue native gel, the detergent solubilized MsbA migrated through the gel and was apparent as a single band (Figure 3.2 E, lane 1). Blue-native PAGE unlike clear-native PAGE uses the anionic Blue G dye which coats proteins and protein complexes due to its hydrophobic properties, resulting in negatively charged protein surfaces. Such surface coated proteins have a much reduced tendency to aggregate and become water-soluble because of their negatively charged surfaces. Thus, membrane proteins can migrate into the blue-native PAGE and are separated based on their molecular sizes once they are coated with the dye. The soluble nanodiscs containing MsbA with MSP1 or MSP3 migrated as expected; Nd-MsbA with MSP3 migrated more slowly than Nd-MsbA with MSP1 because MSP3 is larger than MSP1. (Figure 3.2 E, compare lane 2 and 5).

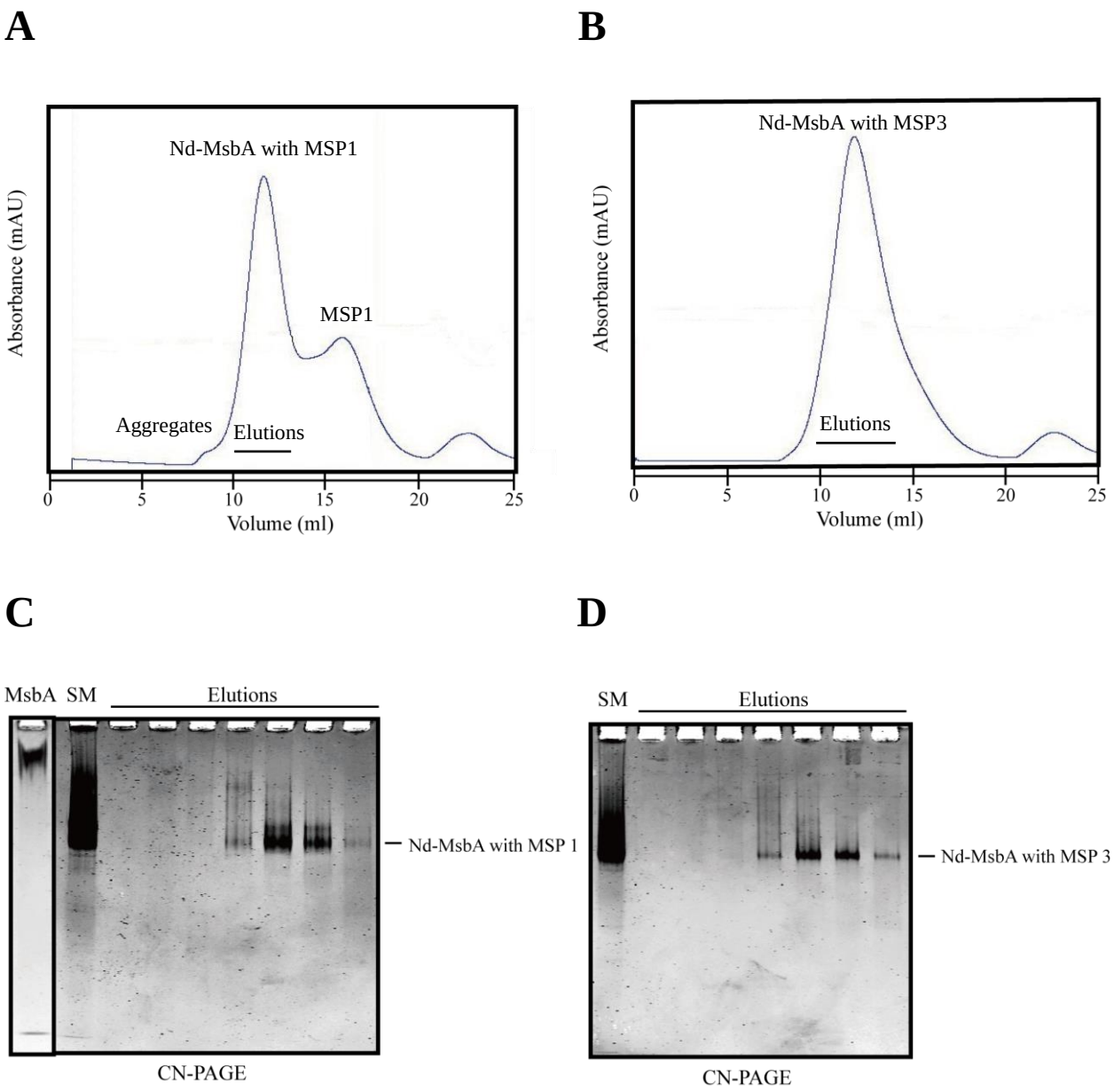
A
Nd-MsbA with MSP1
Absorbance (mAU)
MSP1
Aggregates
Elutions
0
5
10
15
20
25
Volume (ml)
B
Nd-MsbA with MSP3
Absorbance (mAU)
Elutions
0
5
10
15
20
25
Volume (ml)
C
MsbA
SM
Elutions
Nd-MsbA with MSP 1
CN-PAGE
D
SM
Elutions
Nd-MsbA with MSP 3
CN-PAGE

E

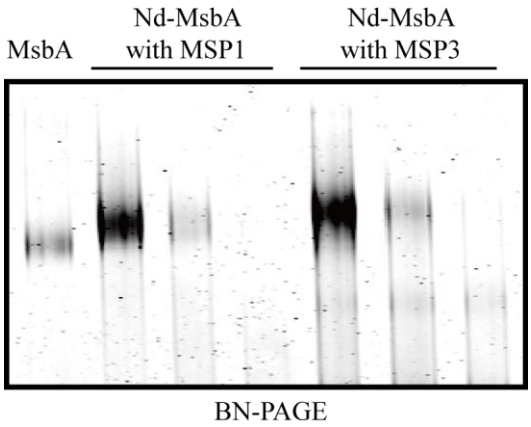

Figure 3.2 Size exclusion chromatography and native-PAGE analysis of Nd-MsbA
Nanodisc reconstitutions were performed as indicated in section 2.1.8. Nd-MsbA reconstituted with MSP1 (A) or MSP3 (B) was subjected to size exclusion chromatography using Superdex^{TM} 200 HR 10/300 column. C. Pure Nd-MsbA with MSP1 of gel filtration fractions was analyzed by CN-PAGE. D. Pure Nd-MsbA with MSP3 of gel filtration fractions was analyzed by CN-PAGE. E. BN-PAGE analysis of pure Nd-MsbA with MSP1 and MSP3.

3.1.3 ATPase activity of Nd-MsbA

It has been demonstrated from previous research that ATPase activity is used to monitor the functionality of MsbA and other ABC transporters (53-56); in this study, ATPase activities of MsbA and Nd-MsbA were therefore analyzed.

The release of orthophosphate upon the hydrolysis of ATP by MsbA was directly monitored using a photo-colorimetric method. The formation of green molybdophosphoric acid complex between malachite green molybdate and free orthophosphate in one to one ratio was

measured by a spectrophotometer at 660 nm. At each time point, 0, 1, 3, 5, 7, and 10 min, the amount of orthophosphate released per mg of protein, MsbA, was measured, and the values were plotted against time. The rate of ATP hydrolysis (nmol of phosphate/mg of protein/min) was then determined from the slope of the graph.

It was found that MsbA in detergent hydrolyzed ATP at a rate of ~250 nmol Pi/min/mg (Figure 3.3, lane1), yet functionally competent homodimer of MsbA reconstituted into a nanodisc each with MSP1 or MSP3 hydrolyzed ATP at a rate of 2000 and 1800 nmol Pi/min/mg respectively (Figure 3.3, lane2 and 3), which reveals an adverse effect of detergent. The smaller nanodiscs with MSP1 had slightly higher ATPase activity than nanodiscs with MSP3. The ATPase activities obtained here were higher than those (2 – 1300 nmol/mg/min) reported by other groups. (47, 55, 57).

Enzymatic activity of both Nd-MsbA with MSP1 and MSP3 was inhibited when 2 mM vanadate was added. As supported by a number of studies of ATPase inhibition by vanadate, catalytic activities of Nd-MsbA were hampered by vanadate as well (47, 58) (Figure 3.3, lane 4 and 5)

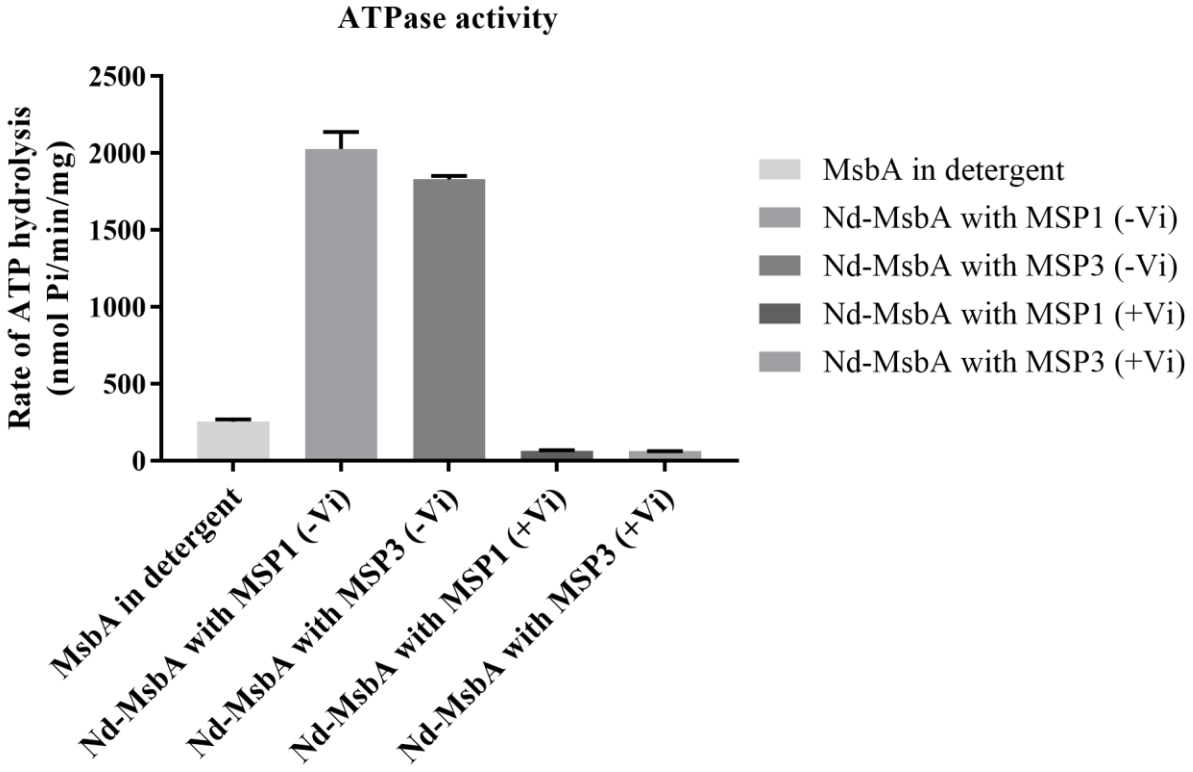

Figure 3.3 ATPase activity of Nd-MsbA
Lane 1: MsbA in detergent. Lane 2: MsbA reconstituted into nanodisc with MSP1. Lane 3: MsbA nanodisc with MSP3. Lane 4 and 5: Nd-MsbA with MSP1 and MSP3 respectively in the presence of 2 mM vanadate. ATPase activity of MsbA was measured as stated in section 2.1.11. The reported values were derived from 3 independent experiments.

3.2 Expression and characterization of MsbA fusion constructs

3.2.1 Expression and localization test of MsbA fusion constructs

Expression of the fusion constructs, His_7-MBP-MSP1-MsbA and His_7-MBP-MSP3-MsbA was tested by loading whole cell lysate at each time point: before induction and after 1, 2, and 3 h of induction on SDS-PAGE. The fusion constructs were well expressed after induction with 100

μM IPTG as shown by a distinct band which appeared after induction, the band intensity being augmented with longer induction times (Figure 3.4 A, B and D). Both fusion constructs migrated as expected for their estimated molecular sizes of about 130 kDa and 140 kDa for the MSP1 and MSP3 fusion constructs, respectively. Since the fusion constructs contained histidine tags at their N-termini, their expression was confirmed by western blotting using an anti-His primary antibody. A typical western blot image is shown for His_7-MBP-MSP1-MsbA (Figure 3.4 B).

To test the extent to which fusion constructs were expressed as soluble proteins aliquots of inclusion bodies, insoluble and soluble fractions from the whole cell lysate were analyzed by SDS-PAGE. Although significant amount of fusion constructs were obtained in the soluble fraction (~20-30 % of total expressed fusion protein), most of the expressed constructs were pelleted in the insoluble fractions (~70-80 % of total expressed fusion protein) (Figure 3.4 A and D, lane 7 and 8). Most of the fusion constructs from the insoluble fractions were extracted by overnight solubilization by triton X-100 (final concentration of 0.5 % w/v) as shown by predominant band (Figure 3.4 C and E, lane 2 and 3). Any residual non-solubilized materials were further treated with SDS solution.

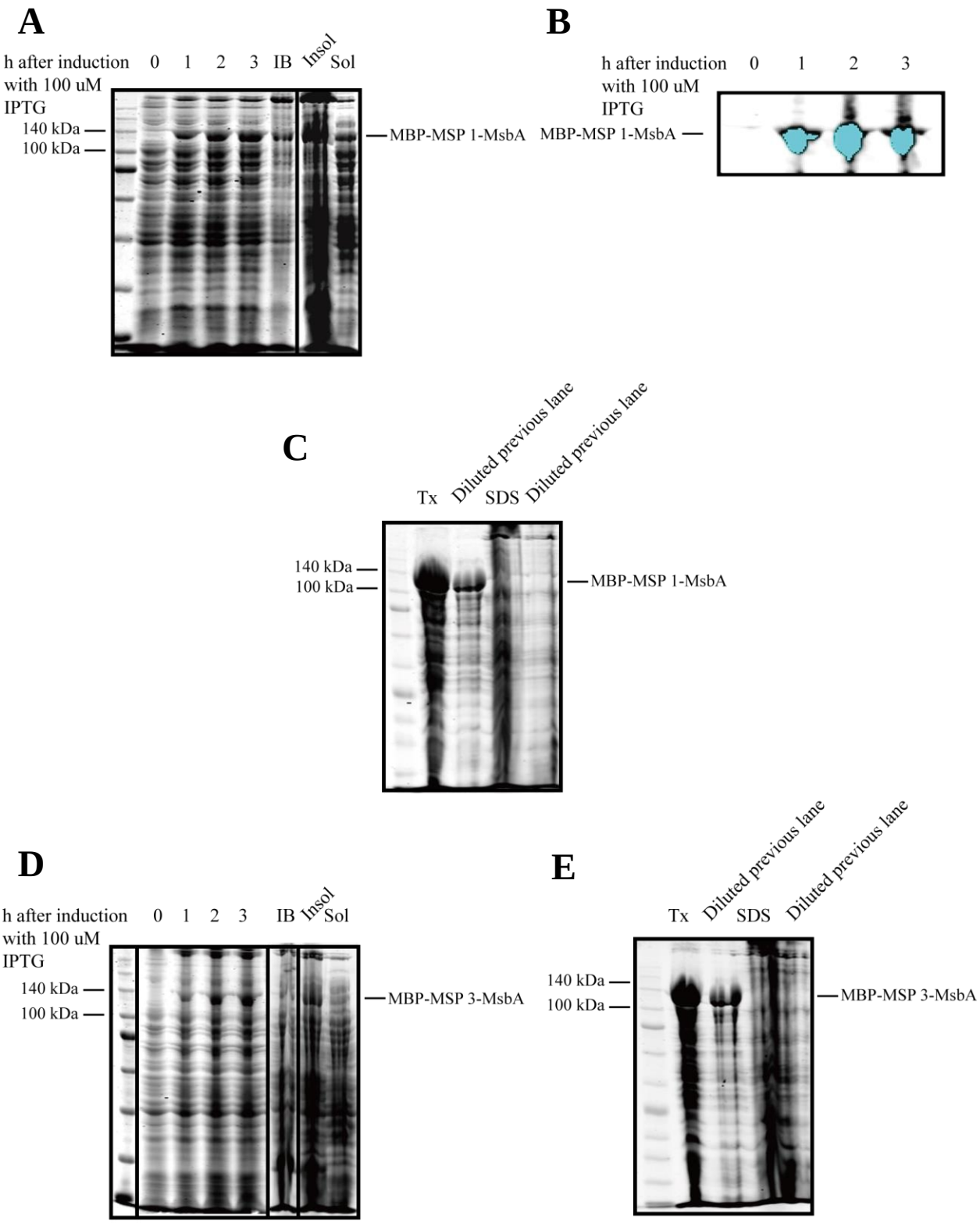
A
h after induction with 100 uM IPTG
0
1
2
3
IB
Insol
Sol
140 kDa
100 kDa
MBP-MSP 1-MsbA
B
h after induction with 100 uM IPTG
0
1
2
3
MBP-MSP 1-MsbA
C
Tx
Diluted previous lane
SDS
Diluted previous lane
140 kDa
100 kDa
MBP-MSP 1-MsbA
D
h after induction with 100 uM IPTG
0
1
2
3
IB
Insol
Sol
140 kDa
100 kDa
MBP-MSP 3-MsbA
E
Tx
Diluted previous lane
SDS
Diluted previous lane
140 kDa
100 kDa
MBP-MSP 3-MsbA

Figure 3.4 Expression and localization of MsbA fusion constructs
The fusion constructs, MBP-MSP1-MsbA and MBP-MSP3-MsbA were expressed in C43 cells. A. Protein expression (MBP-MSP1-MsbA) was tested after 1, 2, and 3 hours of induction with 100 μM IPTG using whole cell extracts (1, 2, 3 hr) or inclusion bodies (IB) or insoluble (Insol) or soluble (Sol) extracts obtained at 3h. B. Expression of MBP-MSP1-MsbA was confirmed by western blot with anti-His primary antibody. C. Insoluble fraction containing the construct, MBP-MSP1-MsbA was solubilized by 0.5 % Tx-100 and loaded with its diluted aliquot onto SDS-PAGE. Triton-X100-insoluble fraction was further treated with 2 % SDS. SDS solubilized fraction and its diluted aliquot were visualized on SDS-PAGE. D. Protein expression (MBP-MSP3-MsbA) was tested after 1, 2, and 3 hours of induction with 100 μM IPTG using whole cell extracts (1, 2, 3 hr) or inclusion bodies (IB) or insoluble (Insol) or soluble (Sol) extracts obtained at 3h. E. Insoluble fraction containing the construct, MBP-MSP3-MsbA was solubilized by 0.5 % Tx-100. Triton-X100-solubilized material and its diluted aliquot were loaded onto SDS-PAGE. Triton-X100-insoluble fraction was further treated with 2 % SDS. SDS solubilized fraction and its diluted aliquot were visualized on SDS-PAGE.

3.2.2 Amylose column purification and native-PAGE analysis

His_7-MBP-MSP1-MsbA and His_7-MBP-MSP3-MsbA were purified as described in the methods section 2.2.7. Most of the fusion constructs were eluted in the first three fractions from amylose column for both purifications of soluble and insoluble fractions. They migrated at around 130 or 140 kDa for MSP1 and MSP3 fusion constructs respectively on SDS-PAGE. For soluble fraction purification, significant amount of maltose binding protein was co-eluted with the fusion constructs as marked and labeled (Figure 3.5 A and B) yet for insoluble fraction purification, as expected, almost no maltose binding protein was co-eluted as shown by both SDS-PAGE and western blot (Figure 3.6 A, B, and C). The co-purified MBP from soluble fraction was not detected by western blot, indicating that it was not a cleaved N-terminal MBP from the fusion constructs (data not shown). The fractions eluted in 0.05 % Tx-100 from soluble fraction amylose purifications were analyzed on both colorless native and blue native gels where both fusion

constructs and co-purified MBP run as distinct single bands (Figure 3.5 C and D). The fractions from insoluble fraction amylose purifications were also loaded on both CN-PAGE and BN-PAGE where fusion constructs appeared as a single band (Figure 3.6 D and E). It was expected that the fusion construct with MSP3 migrated slower than that with MSP1 because of its higher molecular weight. A typical preparation yielded ~1 mg of purified fusion protein from soluble fraction and ~2.2 mg from insoluble fraction from total 500 ml of cell cultures.

A

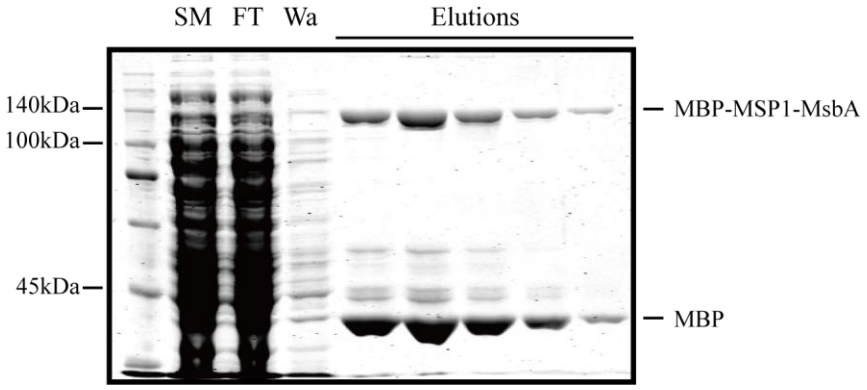
SM
FT
Wa
Elutions
140kDa
100kDa
45kDa
MBP-MSP1-MsbA
MBP

B

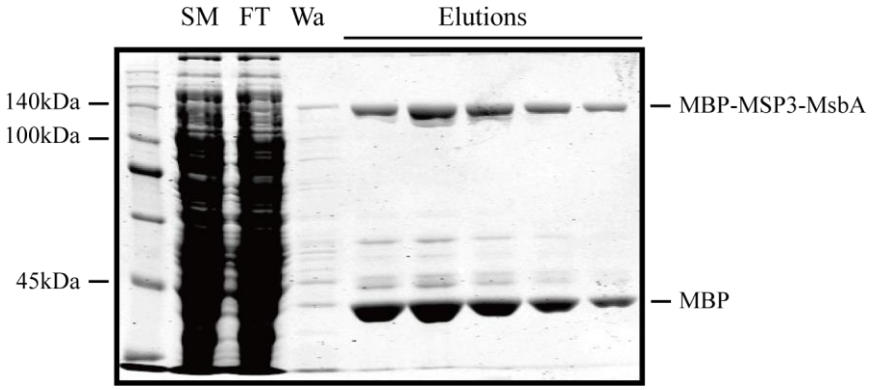
SM
FT
Wa
Elutions
140kDa
100kDa
45kDa
MBP-MSP3-MsbA
MBP

C

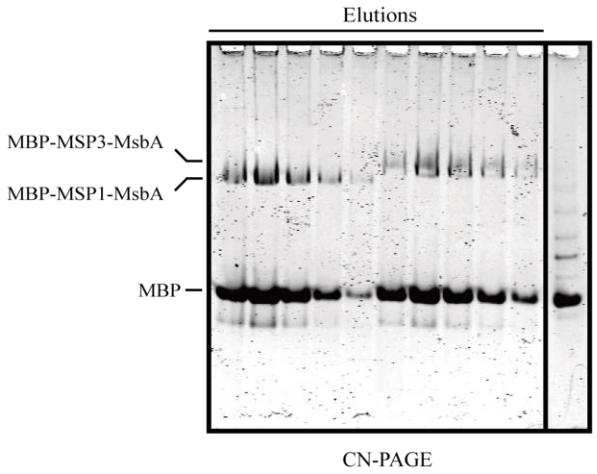
Elutions
MBP-MSP3-MsbA
MBP-MSP1-MsbA
MBP
CN-PAGE

D

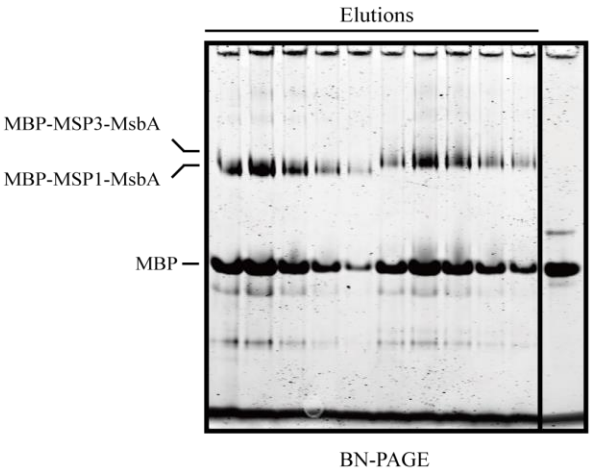
Elutions
MBP-MSP3-MsbA
MBP-MSP1-MsbA
MBP
BN-PAGE

Figure 3.5 Amylose purification of the fusion constructs from soluble fraction

A. SDS-PAGE analysis of starting material (SM), flow through (FT), wash (Wa), and elution fractions from amylose purification of MBP-MSP1-MsbA fusion construct. The fusion construct was loaded onto the amylose column and eluted in 20 mM maltose and detergent. Five 1 ml fractions were collected. B. SDS-PAGE analysis of starting material (SM), flow through (FT), wash (Wa), and elution fractions from amylose purification of MBP-MSP3-MsbA fusion construct. The fusion construct was loaded onto the amylose column and eluted in 20 mM maltose and detergent. Five 1 ml fractions were collected. C. Clear-native PAGE analysis of elution fractions of MBP-MSP1-MsbA and MBP-MSP3-MsbA fusion constructs from amylose purification. The last lane represents free MBP as a loading control. D. Blue-native PAGE analysis of elution fractions of MBP-MSP1-MsbA and MBP-MSP3-MsbA fusion constructs from amylose purification. The last lane represents free MBP as a loading control.

A

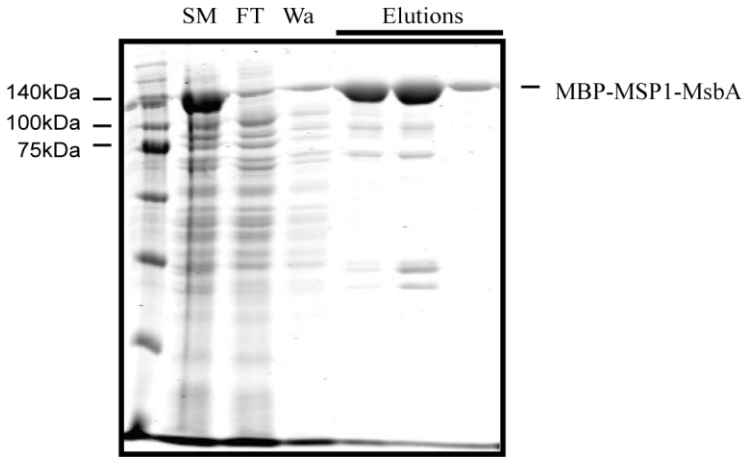
SM
FT
Wa
Elutions
140kDa
100kDa
75kDa
MBP-MSP1-MsbA

B

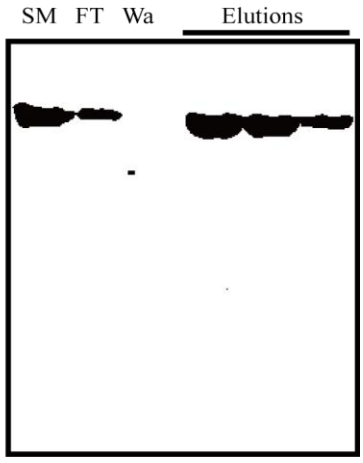
SM
FT
Wa
Elutions

C

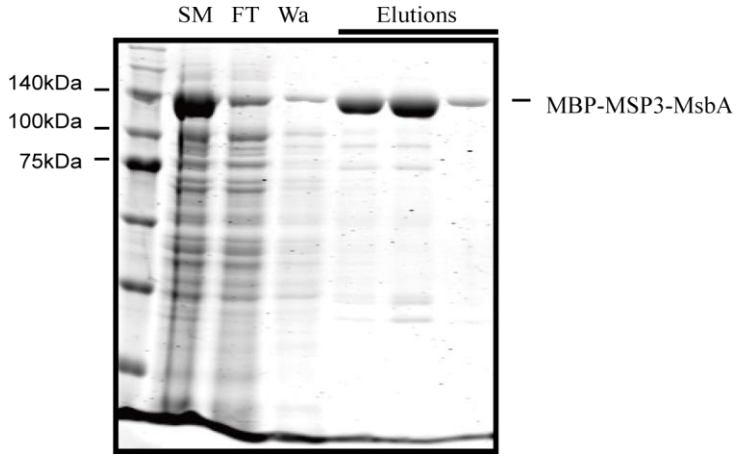
SM
FT
Wa
Elutions
140kDa
100kDa
75kDa
MBP-MSP3-MsbA

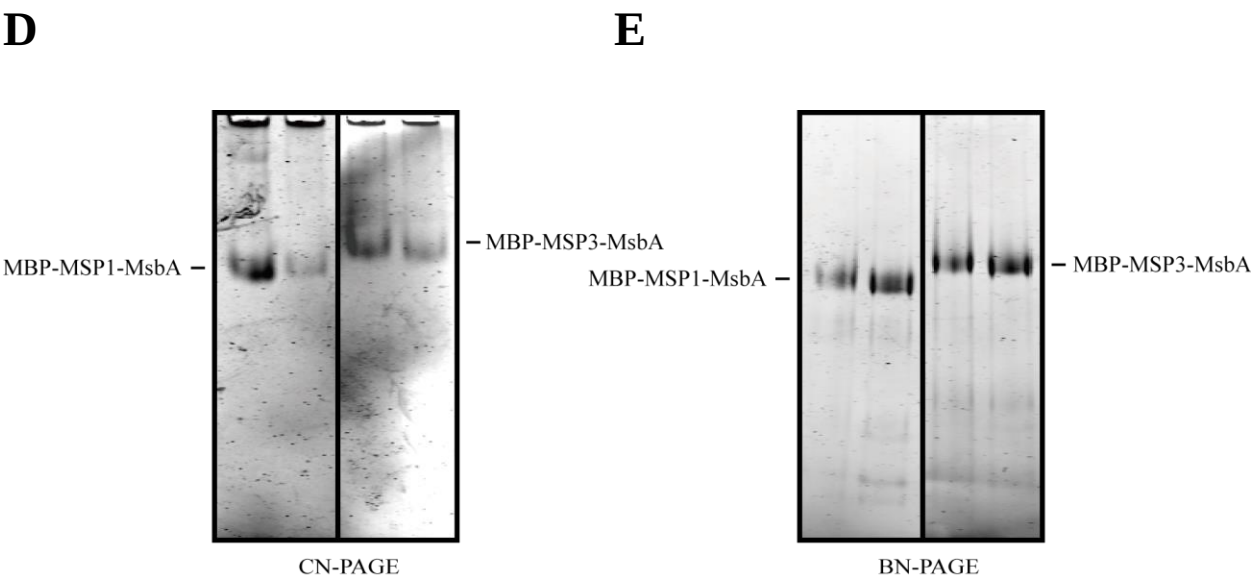

Figure 3.6 Amylose purification of the fusion constructs from insoluble fraction
A. SDS-PAGE analysis of starting material (SM), flow through (FT), wash (Wa), and elution fractions from amylose purification of MBP-MSP1-MsbA fusion construct. The fusion construct was loaded onto the amylose column and eluted in 20 mM maltose and detergent. Three 1 ml fractions were collected. B. Western blot image of A. C. SDS-PAGE analysis of starting material (SM), flow through (FT), wash (Wa), and elution fractions from amylose purification of MBP-MSP3-MsbA fusion construct. The fusion construct was loaded onto the amylose column and eluted in 20 mM maltose and detergent. Three 1 ml fractions were collected. D. Clear-native PAGE analysis of elution fractions of fusion constructs from amylose purification. E. Blue-native PAGE analysis of elution fractions of fusion constructs from amylose purification.

3.2.3 Size exclusion chromatography and native-PAGE analysis

The fusion constructs were further purified by size exclusion chromatography to remove co-purified MBP and other contaminants, to examine whether the fusion constructs remained soluble after washing out detergent and to determine their approximate molecular sizes. Elution from amylose purification was injected into the Superdex^{TM} 200 HR 10/300 column equilibrated in detergent free buffer. Both fusion constructs with MSP1 and MSP3 remained soluble in a detergent free environment and had an estimated molecular weight of dimeric MsbA fusion. Results are shown only for MBP-MSP1-MsbA fusion construct. The elution profile of the fusion construct from the soluble fraction shows three peaks; the first peak corresponds to aggregates, the second peak to the fusion construct and the last peak to MBP (Figure 3.7 A). Fractions corresponding to the second peak were analyzed by both SDS-PAGE and clear native gel, which confirmed that the second peak represents the soluble fusion construct (Figure 3.7 B and C). The gel filtration profile of the fusion construct from the insoluble fraction shows a major peak followed by a small peak; the major peak corresponds to the fusion construct and the second peak at around 16 ml represents any contaminants (Figure 3.8 A). The major peak was confirmed to represent the fusion construct as its corresponding fractions contain pure fusion construct shown by both SDS-PAGE and blue-native PAGE (Figure 3.8 B and C). A little bump at the start of the major peak is aggregated proteins.

A

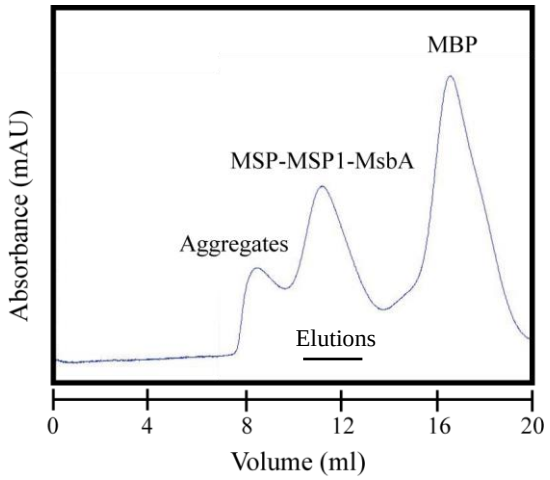
MBP
MSP-MSP1-MsbA
Aggregates
Elutions
Absorbance (mAU)
0
4
8
12
16
20
Volume (ml)

B

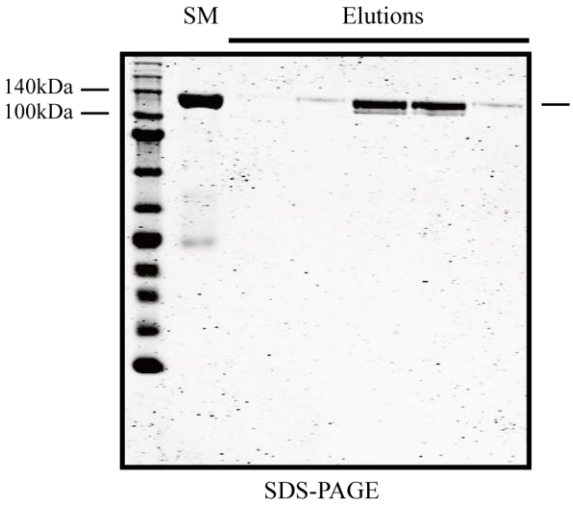
SM
Elutions
140kDa
100kDa
MBP-MSP1-MsbA
SDS-PAGE

C

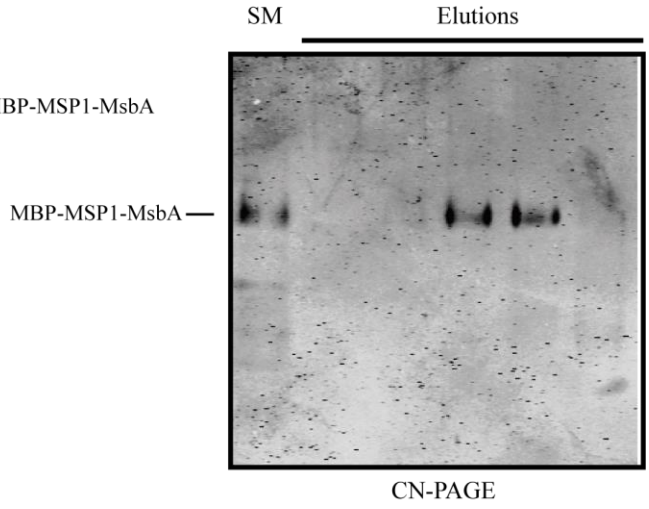
SM
Elutions
MBP-MSP1-MsbA
CN-PAGE

Figure 3.7 Size exclusion chromatography of MBP-MSP1-MsbA purified from soluble fraction.

A. A purified fraction of fusion construct, MBP-MSP1-MsbA from amylose purification of soluble fraction was injected onto a Superdex^{TM} 200 HR 10/300 column equilibrated in buffer C (20 mM Tris-HCl pH 7.9, 200 mM NaCl, 10 % v/v glycerol and 1 mM DTT). B. SDS-PAGE analysis of SM (starting material) and elution fractions of gel filtration, corresponding to the second peak. C. Clear-native PAGE analysis of SM (starting material) and gel filtration fractions, corresponding to the second peak.

A

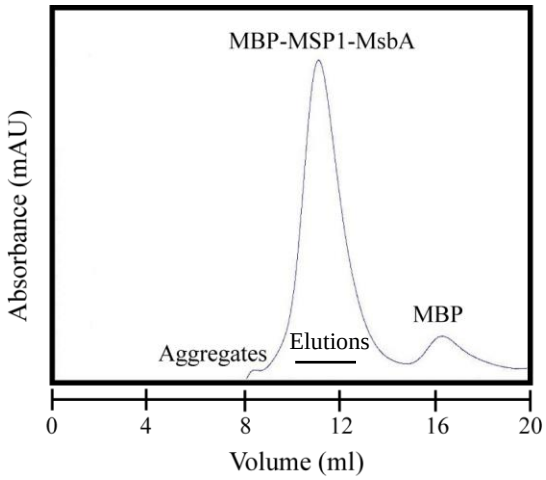
MBP-MSP1-MsbA
Absorbance (mAU)
MBP
Aggregates
Elutions
0
4
8
12
16
20
Volume (ml)

B

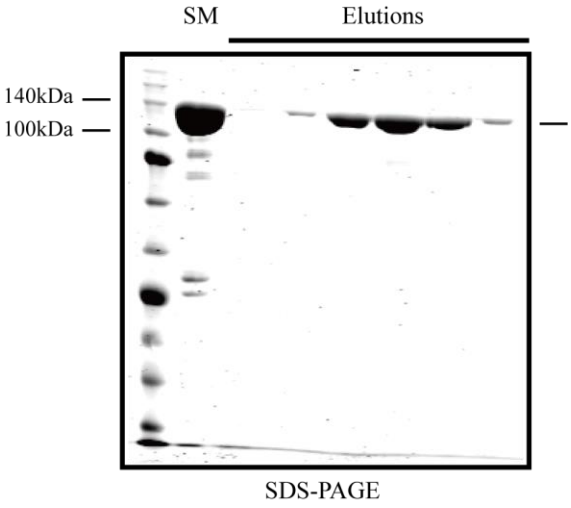
SM
Elutions
140kDa
100kDa
MBP-MSP1-MsbA
SDS-PAGE

C

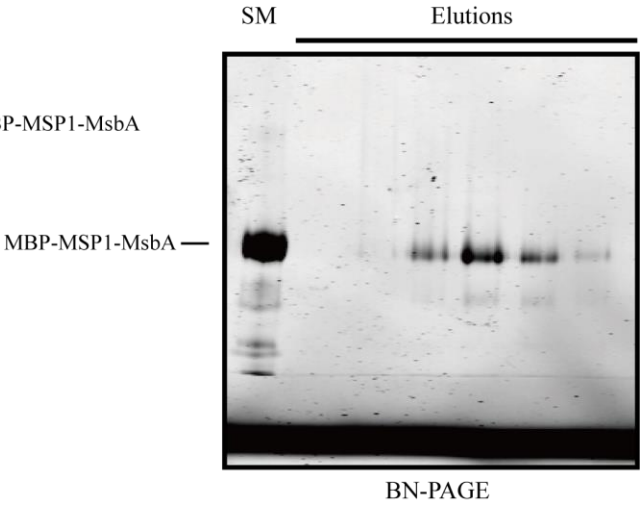
SM
Elutions
MBP-MSP1-MsbA
BN-PAGE

Figure 3.8 Size exclusion chromatography of MBP-MSP1-MsbA purified from insoluble fraction

A. A purified fraction of fusion construct, MBP-MSP1-MsbA from amylose purification of insoluble fraction was injected onto a Superdex^{TM} 200 HR 10/300 column equilibrated in buffer C (20 mM Tris-HCl pH 7.9, 200 mM NaCl, 10 % v/v glycerol and 1 mM DTT). B. SDS-PAGE analysis of SM (starting material) and elution fractions, corresponding to the major peak. C. Blue-native PAGE analysis of SM (starting material) and gel filtration fractions, corresponding to the major peak.

3.2.4 ATPase activity of the fusion constructs

To test whether the purified fusion constructs were functionally comparable with in vitro Nd-MsbA, their biological activities were measured and analyzed as described below.

The release of orthophosphate upon the hydrolysis of ATP by MsbA was directly measured by photo-colorimetric method using malachite green method. Rates of hydrolysis were determined by plotting the nanomoles of Pi released per milligram of protein versus time.

It was found that both of the fusion constructs, MBP-MSP1-MsbA and MBP-MSP3-MsbA were able to preserve catalytic activities, with a rate of 1600 and 1000 nmol Pi/min/mg respectively (Figure 3.9, lane 1 and 2). The difference of the enzymatic rates between two fusion constructs was greater than that between in vitro Nd-MsbA with MSP1 and MSP3. The smaller fusion construct with MSP1 sustained much higher ATPase activity than that with MSP3.

For ATPase inhibition assay, 2 mM of Vi was added to the reaction mixture. It was revealed that vanadate inhibited the ATPase activities of both fusion constructs by more than 90 % up to ~50 nmol Pi/min/mg (Figure 3.9, lane 3 and 4).

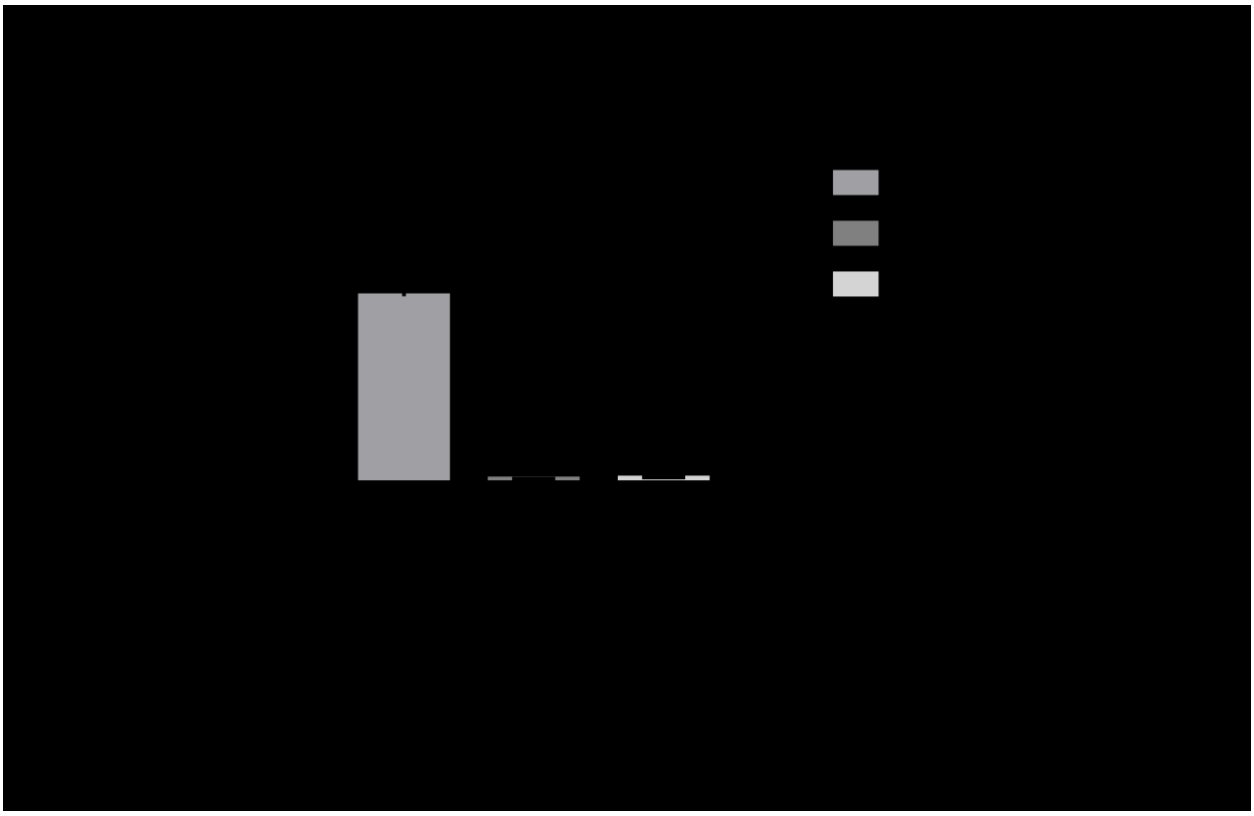

Figure 3.9 ATPase activity of MsbA fusion constructs in detergent-free solution
Lane 1: MBP-MSP1-MsbA. Lane 2: MBP-MSP3-MsbA. Lane 3: MBP-MSP1-MsbA in the presence of 2 mM vanadate. Lane 4: MBP-MSP3-MsbA with 2 mM vanadate. ATPase activity of MsbA was measured as stated in section 2.1.11. The reported values were derived from 3 independent experiments.

3.2.5 Thin layer chromatography

Lipids associated with the purified proteins were analyzed by thin layer chromatography as indicated in section 2.2.8. Briefly, lipids were extracted by chloroform-methanol solvent system, separated on TLC plate, and analyzed by Image J densitometry. At the initial step of extraction process, radiolabeled lipids were added to each sample to be used as an internal standard for lipid extraction to take an account of total loss of lipids for normalization at the end of analysis.

The relative amount of lipids in each sample was plotted on the graph as shown in Figure 3.10. Purified MsbA in detergent and Nd-MsbA contained about 80 and 73 % relative amount of lipids respectively (Figure 3.10, lane 1 and 2). Although detergent purified MsbA was reconstituted into nanodisc without addition of any lipids, the relative amount of lipids in Nd-MsbA determined by TLC experiment is likely from the lipids that were initially associated with purified MsbA and incorporated into the nanodisc during reconstitution process.

The amounts of lipids between purified fusion constructs from soluble fraction in the absence and presence of detergents were compared in order to ascertain if the fusion constructs are associated with any lipids. In lane 3 of Figure 3.10, the fusion construct, MBP-MSP3-MsbA purified from soluble fraction in the absence of detergent had the largest amount of lipids, while purified MBP-MSP3-MsbA from soluble fraction in the presence of detergent had significantly lower residual amounts of lipids as shown in lane 5. The results support the idea that the fusion construct is initially associated with lipids which are washed out after detergent wash step during purification step. The detergent wash was necessary to have a properly folded soluble fusion construct as the purified fusion construct without detergent was shown as an aggregate on native-PAGE and size exclusion chromatography (Appendix B), and had no ATP hydrolysis activity (data not shown). The results that the fusion protein was associated with lipids and appeared as an aggregate before the treatment with detergent indicate that detergent was necessary to promote proper refolding process of the fusion construct while washing out extra lipids that may contribute the formation of large lipid associated aggregate.

Each purified MBP-MSP3-MsbA fusion protein with and without detergent was further analyzed by Superdex^{TM} 200 that was equilibrated in detergent free buffer. Each fraction from gel

filtrations was subjected to TLC experiment for its lipid association. As shown in lane 4, the purified fusion protein without detergent had prominent decrease in the amount of lipid after the gel filtration as any lipid aggregates were removed during gel filtration. On the other hand, the purified fusion protein with detergent in lane 6 showed only subtle change in the amount of lipid after the gel filtration step, which would be due to the pre-detergent wash step during amylose purification process that removed excess amount of lipids beforehand.

Figure 3.10 Lipids association of the fusion construct, MBP-MSP3-MsbA
Lipids in each protein sample were extracted and separated on TLC plate. The intensity of spots for lipids was normalized and analyzed by Image J, and relative amount of lipids in each sample was quantified in percentage. Radiolabeled lipids were used as an internal standard to track the loss of lipids during experimental process. Lane 1: detergent solubilized MsbA. Lane 2: Nd-MsbA comprised of MSP3. Lane 3: MBP-MSP3-MsbA fusion protein purified from soluble fraction without detergent by amylose column. Lane 4: post gel filtration fraction of the sample of lane 3. Lane 5: MBP-MSP3-MsbA fusion protein purified from soluble fraction in the presence of detergent by amylose column. Lane 6: post gel filtration fraction of the sample of lane 5. The reported values were derived from 3 independent experiments.

Chapter 4: Discussion

4.1 MsbA and Nd-MsbA

4.1.1 Expression and purification of MsbA

Escherichia coli bacterial expression system has been a benchmark for comparing various expression platforms and a successful vehicle for over-expression of prokaryotic and eukaryotic proteins (59). However, it is general observation that over-expression of membrane protein in sufficient quantities for in vitro functional and structural studies has been challenging because of the toxicity of overexpression. In this study, for expression of recombinant membrane protein, His_7-MsbA, a mutant host strain *E.coli* C43 (DE3) was used. The expression level of MsbA in C43 (DE3) cell was higher than that of MsbA in BL21 (DE3) host strain; the global amount of MsbA produced and purified per liter of culture was significantly greater in C43 (DE3) cell than BL21 (DE3) (data not shown). It has been reported that the host strains C41 (DE3) and C43 (DE3) are effective in sustaining expression of some toxic membrane proteins because of the mutations in the *lac*UV5 promoter governing expression of T7 RNA polymerase (60). These mutations result in the production of much lower amounts of T7 RNA polymerase, leading to lower production rates of the mRNA for the membrane protein, which would subsequently ensure that the capacity of the membrane protein insertion machinery, Sec translocon is sufficient to integrate the overexpressed protein into the membrane (61).

4.1.2 Nanodisc reconstitution of MsbA

More than sufficient amounts of MsbA purified from a Ni-NTA column was reconstituted into nanodiscs with MSP1 or MSP3 which became highly pure after gel filtration as shown by native-PAGE analysis. The migration of proteins on native-PAGE is dictated by either the protein's pI or molecular weight, depending on the presence of negatively charged Coomassie-dye. Blue-native PAGE is supplemented with this negatively charged protein-binding dye, Coomassie Brilliant Blue G-250 which would allow separation of proteins in non-reducing polyacrylamide gradient gels according to their molecular mass while clear-native PAGE requires inherent negative charge of proteins (with pI < 7). Proteins migrate into these gradient gels with decreasing pore size until they reach their specific size-dependent pore-size limit (62). The fact that the purified seven histidine tagged MsbA has theoretical pI of 8.82 and forms an aggregate as detergent micelles are washed away on the migration pathway prevents it from migration on the CN-PAGE, yet with sufficient negative charges on its surface due to the blue Coomassie-dye, its migration is apparent on the BN-PAGE. The soluble Nd-MsbA with MSP1 or MSP3 migrated on CN-PAGE and BN-PAGE. It has been demonstrated that the resolution of CN-PAGE was found to be lower compared to that of BN-PAGE. Molecular masses are not easily determined by CN-PAGE unless the protein has pI below 5.4 (63). It is conspicuous to observe the difference in migration between MsbA and Nd-MsbA such that Nd-MsbA migrated to higher position on the gel than MsbA for additional weight of MSP molecules. The resolution is so strong that it is possible to observe differences as small as 20 kDa by comparing Nd-MsbA including MSP1 with Nd-MsbA including MSP3.

4.1.3 ATPase activity of MsbA and Nd-MsbA

Under the experimental conditions tested (10 mM magnesium, 2 mM ATP and pH 8) the rate of ATP hydrolysis of MsbA in detergent micelles (~250 nmol Pi/min/mg) was about 10 times higher than that of reported values (47, 57) (Figure 3.3). It was demonstrated that typically low basal ATPase activity of detergent solubilized MsbA was greatly stimulated and stabilized by addition of lipids, which would suggest that MsbA purified under the condition stated in this thesis contains higher amount of lipids than that studied by other researchers. It can be suggested that the higher ATPase activity measured in this set of experimental condition might be due to any residual *E.coli* lipids in detergent-lipid micelles after purification. The presence of lipids in detergent purified MsbA was verified by TLC lipid extraction experiment (Figure 3.10).

It was demonstrated that catalytic activity of MsbA was strongly affected by nanodisc reconstitution; nanodisc MsbA has much higher capacity of hydrolyzing ATP than detergent purified MsbA with an increase of 8 fold, supporting the fact that native-like lipid bilayer environment is critical for functionality of membrane proteins (Figure 3.3). The removal of detergent during the nanodisc reconstitution abolishes detrimental effect of detergent on the function of membrane proteins as well. The environmental condition in which MsbA is sequestered by the lipid bilayer and amphipathic molecules in the absence of detergent greatly increased its ability to hydrolyze ATP.

Additional characterization of the ATPase activity of MsbA that showed the effects of known inhibitor, vanadate, supported the notion that vanadate is a potent inhibitor of the P-glycoprotein ATPase. Vanadate is thought to block the catalytic cycle of the transporter by forming a noncovalent complex with MgADP at the site of ATP hydrolysis (64). Doerrler et al. (47) had

proven that the ATPase activity of reconstituted MsbA into proteoliposome was inhibited, which is supported by the result in this thesis.

4.2 MsbA fusion construct, His_7-MBP-MSP-MsbA

4.2.1 Expression and purification of the fusion construct

It was found that the fusion constructs, MBP-MSP1-MsbA and MBP-MSP3-MsbA were successfully expressed (~4-5 times more than MsbA alone), yet fractionation of cell lysates indicated that most of them were localized in membrane fraction although significant amounts were in soluble fraction (Figure 3.4). Detergent treatment was necessary in order to produce soluble form of the fusion protein from soluble fraction. The fact that this fusion protein even from soluble fraction forms aggregates (Appendix B) suggested that the initially synthesized fusion protein is associated with large number of lipid molecules and perhaps not correctly folded, forming lipid aggregates in various sizes. The lipid aggregates in smaller size remains in the supernatant of high speed centrifugation while the larger size would be pelleted in membrane fraction. Once these lipid aggregates are treated with detergent and subjected to purification steps by amylose column and Superdex^{TM} 200, the lipids associated with the fusion protein are washed away and the fusion protein is refolded into a functionally active form. It was demonstrated that the fusion protein purified in the absence of detergent was eluted as an aggregate (Appendix B) and had no enzymatic activity. Also, the presence of lipids in fusion protein was proven by lipid extraction experiment that further reinforces the hypothesis of formation of lipid aggregates (Figure 3.10). The mechanism behind the formation of lipid aggregates may be explained by the nature of the pre-cursor protein, apolipoprotein A-I, of membrane scaffold protein which has high

tendency to associate with lipids. When apolipoprotein A-I forms high density lipoprotein, it avidly binds phospholipid molecules and organizes them into soluble structure to satisfy thermodynamic stability with a major driving force of negative free energy gained by the transfer of hydrophobic residues from water to the interior of a phospholipid bilayer (65). The membrane scaffold protein which is the derivative of ApoA-I is proven to be flexible (18). Morgan et al. (18) used hydrogen exchange mass spectrometry to probe the structure and dynamics of the scaffold protein in the absence and presence of lipids, and it was demonstrated that MSP underwent a gross structural rearrangement and deuteration of MSP was decreased upon lipid-association. However, it was found that MSP in nanodiscs still constituted dynamic conformational changes and became significantly deuterated despite having a high percentage of helical content and hydrophobic interactions with the lipids (18). It is possible that the fusion protein grabs *E.coli* lipids in the whole cell lysate after shearing the cells. When stop codon was inserted in MBP-MSP-MsbA fusion construct right before MsbA to produce only MBP-MSP protein, the localization test showed that significant amount of MBP-MSP was found in insoluble fraction and recovered in purification step, which implies that MSP is most likely the main contribution to formation of lipid aggregates (Appendix C). However, the possibility that it picks up the lipids during its translation could not be excluded. The order of synthesizing each protein cannot be overlooked as a matter of lipid aggregation formation. Mizrachi et al. recently showed that the fusion strategy with the backbone structure of the N-terminal decoy protein, MBP – membrane protein – truncated ApoA-I at the C-terminus had successfully solubilized membrane proteins in vivo without the need of detergent (66).

4.2.2 ATPase activity and its correlation with lipids association

The functionality of these fusion proteins was verified with their ATPase activity. The result that shows MBP-MSP1-MsbA represents almost twice higher ATPase activity than MBP-MSP3-MsbA (Figure 3.9) agrees with the result of Kawai et al. that showed Nd-MsbA composed of MSP1 was best suited to preserve the enzymatic activity of MsbA than the other Nd-MsbA composed of other longer MSPs; they found that Nd-MsbA with MSP1 had twice higher rate of ATP hydrolysis than that with MSP3, but there was no linear dependence of enzymatic rates as size of nanodisc was increased (57). Moreover, the fusion constructs had the decreased ATPase activities when the inhibitor, vanadate, was present. This additional characterization of the ATPase inhibition assay lends weight on retention of structurally relevant conformation of MsbA fusion constructs as well.

The correlation of enzymatic activity and lipid contents was observed such that the rate of catalytic activity of MsbA depends on the amount of lipids it is associated with. The in vitro Nd-MsbA composed of MSP3 which contains twice as much lipid as the fusion protein, MBP-MSP3-MsbA (compare Figure 3.10, lane 2 with 6) hydrolyzes ATP almost twice much faster than the fusion protein (compare Figure 3.3, lane 3 with Figure 3.9, lane 2) as it was demonstrated by Doerrler et al. (47) that lipids stimulates ATPase activity of MsbA. It is already supported by a number of papers that for many ABC transporters their endogenous ATPase activity is specifically stimulated by interaction with the transported substrate (67-69).

Overall taken together, the results indicate that it was feasible to produce a soluble membrane protein in an active form in vivo. Although we did not expect the need for detergent in the purification step, the results that the final product remains soluble and that it retains a

structurally and functionally relevant conformation provide an optimistic prospect of the strategy. Although there are number of factors to be considered when designing a fusion construct – such as constraints between each protein and order of synthesis – it can be an affordable and facile method to be applied to various other targets at a minimal cost and effort.

Chapter 5: Conclusion

5.1 Recapitulation of the thesis

Membrane proteins perform key functions in regulating the physiological state of the cell. Their essential roles in the cell promote development of advanced techniques to enable structural and functional studies. Yet, there are still limitations and hindrances in studying them for difficulties associated in dealing with their hydrophobic transmembrane domain. The fusion strategy which takes the advantage of amphipathic membrane scaffold protein has been applied to solubilize *E. coli* membrane protein, MsbA in vivo and it was successful that MsbA was produced in soluble and functionally competent form. The MBP-MSP-MsbA fusion protein passed the critical functional capacity, the ability to hydrolyze ATP, and its enzymatic activity was inhibited in the presence of vanadate.

5.2 Future directions

It was recently reported from a group, Mizrachi et al. that this fusion strategy was applicable to solubilize various small membrane proteins (66). The thesis has investigated the validation of this strategy to much larger membrane protein. In order to further substantiate the strategy, application to wide range of membrane proteins with different size and topology would be necessary. Lastly, it can be an option for challenging membrane proteins that have issues with no expression or instability that hamper future analysis of the proteins.

References

1. Carpenter, E. P., Beis, K., Cameron, A. D., & Iwata, S. (2008). Overcoming the challenges of membrane protein crystallography. *Current opinion in structural biology*, *18*(5), 581-586.
2. Arinaminpathy, Y., Khurana, E., Engelman, D. M., & Gerstein, M. B. (2009). Computational analysis of membrane proteins: the largest class of drug targets. *Drug discovery today*, *14*(23), 1130-1135.
3. Kubicek, J., Block, H., Maertens, B., Spriestersbach, A., & Labahn, J. (2014). Expression and purification of membrane proteins. *Methods in enzymology*, *541* (FZJ-2014-02986), 117-140.
4. Bayburt, T. H., & Sligar, S. G. (2010). Membrane protein assembly into Nanodiscs. *FEBS letters*, *584*(9), 1721-1727.
5. Seddon, A. M., Curnow, P., & Booth, P. J. (2004). Membrane proteins, lipids and detergents: not just a soap opera. *Biochimica et Biophysica Acta (BBA)-Biomembranes*, *1666*(1), 105-117.
6. Akbarzadeh, A., Rezaei-Sadabady, R., Davaran, S., Joo, S. W., Zarghami, N., Hanifehpour, Y., ... & Nejati-Koshki, K. (2013). Liposome: classification, preparation, and applications. *Nanoscale Res Lett*, *8*(1), 102.
7. Rigaud, J. L. (2002). Membrane proteins: functional and structural studies using reconstituted proteoliposomes and 2-D crystals. *Brazilian journal of medical and biological research*, *35*(7), 753-766.
8. Wang, L., & Tonggu, L. (2015). Membrane protein reconstitution for functional and structural studies. *Science China Life Sciences*, *58*(1), 66-74.
9. Chae, P. S., Laible, P. D., & Gellman, S. H. (2010). Tripod amphiphiles for membrane protein manipulation. *Molecular BioSystems*, *6*(1), 89-94.
10. Popot, J. L. (2010). Amphipols, nanodiscs, and fluorinated surfactants: three nonconventional approaches to studying membrane proteins in aqueous solutions. *Annual review of biochemistry*, *79*, 737-775.
11. Denisov, I. G., Grinkova, Y. V., Lazarides, A. A., & Sligar, S. G. (2004). Directed self-assembly of monodisperse phospholipid bilayer Nanodiscs with controlled size. *Journal of the American Chemical Society*, *126*(11), 3477-3487.
12. Grinkova, Y. V., Denisov, I. G., & Sligar, S. G. (2010). Engineering extended membrane scaffold proteins for self-assembly of soluble nanoscale lipid bilayers. *Protein Engineering Design and Selection*, *23*(11), 843-848.
13. Borch, J., & Hamann, T. (2009). The nanodisc: a novel tool for membrane protein studies. *Biological chemistry*, *390*(8), 805-814.
14. Bayburt, T. H., Grinkova, Y. V., & Sligar, S. G. (2002). Self-assembly of discoidal phospholipid bilayer nanoparticles with membrane scaffold proteins. *Nano Letters*, *2*(8),

853-856.
15. Berg, J. M., Tymoczko, J. L., & Stryer L. (2007). *Biochemistry*. (p.9-10). New York, NY: W. H. Freeman.
16. Frank, P. G., & Marcel, Y. L. (2000). Apolipoprotein AI: structure–function relationships. *Journal of lipid research*, *41*(6), 853-872.
17. Jayaraman, S., Benjwal, S., Gantz, D. L., & Gursky, O. (2010). Effects of cholesterol on thermal stability of discoidal high density lipoproteins. *Journal of lipid research*, *51*(2), 324-333.
18. Morgan, C. R., Hebling, C. M., Rand, K. D., Stafford, D. W., Jorgenson, J. W., & Engen,J. R. (2011). Conformational transitions in the membrane scaffold protein of phospholipid bilayer nanodiscs. *Molecular & Cellular Proteomics*, *10*(9), M111-010876.
19. Ajees, A. A., Anantharamaiah, G. M., Mishra, V. K., Hussain, M. M., & Murthy, H. K. (2006). Crystal structure of human apolipoprotein AI: insights into its protective effect against cardiovascular diseases. *Proceedings of the National Academy of Sciences of the United States of America*, *103*(7), 2126-2131.
20. Borhani, D. W., Rogers, D. P., Engler, J. A., & Brouillette, C. G. (1997). Crystal structure of truncated human apolipoprotein AI suggests a lipid-bound conformation. *Proceedings of the National Academy of Sciences*, *94*(23), 12291-12296.
21. Skar-Gislinge, N., Simonsen, J. B., Mortensen, K., Feidenhans'l, R., Sligar, S. G., Lindberg Møller, B., ... & Arleth, L. (2010). Elliptical structure of phospholipid bilayer nanodiscs encapsulated by scaffold proteins: casting the roles of the lipids and the protein. *Journal of the American Chemical Society*, *132*(39), 13713-13722.
22. Li, Y., Kijac, A. Z., Sligar, S. G., & Rienstra, C. M. (2006). Structural analysis of nanoscale self-assembled discoidal lipid bilayers by solid-state NMR spectroscopy. *Biophysical journal*, *91*(10), 3819-3828.
23. Bouige, P., Laurent, D., Piloyan, L., & Dassa, E. (2002). Phylogenetic and functional classification of ATP-binding cassette (ABC) systems. *Current Protein and Peptide Science*, *3*(5), 541-559.
24. Holland, I. B., & Blight, M. A. (1999). ABC-ATPases, adaptable energy generators fuelling transmembrane movement of a variety of molecules in organisms from bacteria to humans. *Journal of molecular biology*, *293*(2), 381-399.
25. Multidrug resistance ABC transporters. Chang, G. (2003). *FEBS Letters 555*, 102-105.
26. Walker, J. E., Saraste, M., Runswick, M. J., & Gay, N. J. (1982). Distantly related sequences in the alpha-and beta-subunits of ATP synthase, myosin, kinases and other ATP-requiring enzymes and a common nucleotide binding fold. *The EMBO journal*, *1*(8), 945.
27. Bianchet, M. A., Ko, Y. H., Amzel, L. M., & Pedersen, P. L. (1997). Modeling of nucleotide binding domains of ABC transporter proteins based on a F1-ATPase/recA topology: structural model of the nucleotide binding domains of the cystic fibrosis

transmembrane conductance regulator (CFTR). *Journal of bioenergetics and biomembranes*, *29*(5), 503-524.

28. Jones, P. M., & George, A. M. (2004). The ABC transporter structure and mechanism: perspectives on recent research. *Cellular and Molecular Life Sciences CMLS*, *61*(6), 682-699.
29. Jones, P. M., & George, A. M. (2012). Role of the D-loops in allosteric control of ATP hydrolysis in an ABC transporter. *The Journal of Physical Chemistry A*, *116*(11), 3004-3013.
30. Hung, L. W., Wang, I. X., Nikaido, K., Liu, P. Q., Ames, G. F. L., & Kim, S. H. (1998). Crystal structure of the ATP-binding subunit of an ABC transporter. *Nature*, *396*(6712), 703-707.
31. Karpowich, N., Martsinkevich, O., Millen, L., Yuan, Y. R., Dai, P. L., MacVey, K., ... & Hunt, J. F. (2001). Crystal structures of the MJ1267 ATP binding cassette reveal an induced-fit effect at the ATPase active site of an ABC transporter. *Structure*, *9*(7), 571-586.
32. Yuan, Y. R., Blecker, S., Martsinkevich, O., Millen, L., Thomas, P. J., & Hunt, J. F. (2001). The crystal structure of the MJ0796 ATP-binding cassette Implications for the structural consequences of ATP hydrolysis in the active site of an ABC transporter. *Journal of Biological Chemistry*, *276*(34), 32313-32321.
33. Smith, P. C., Karpowich, N., Millen, L., Moody, J. E., Rosen, J., Thomas, P. J., & Hunt, J. F. (2002). ATP binding to the motor domain from an ABC transporter drives formation of a nucleotide sandwich dimer. *Molecular cell*, *10*(1), 139-149.
34. Locher, K. P., Lee, A. T., & Rees, D. C. (2002). The E. coli BtuCD structure: a framework for ABC transporter architecture and mechanism. *Science*, *296*(5570), 1091-1098.
35. Chen, J., Lu, G., Lin, J., Davidson, A. L., & Quiocho, F. A. (2003). A tweezers-like motion of the ATP-binding cassette dimer in an ABC transport cycle. *Molecular cell*, *12*(3), 651-661.
36. Schmitt, L., Benabdelhak, H., Blight, M. A., Holland, I. B., & Stubbs, M. T. (2003). Crystal structure of the nucleotide-binding domain of the ABC-transporter haemolysin B: identification of a variable region within ABC helical domains. *Journal of molecular biology*, *330*(2), 333-342.
37. Karcher, A., Bu, K., Märtens, B., Jansen, R. P., & Hopfner, K. P. (2005). X-ray structure of RLI, an essential twin cassette ABC ATPase involved in ribosome biogenesis and HIV capsid assembly. *Structure*, *13*(4), 649-659.
38. Lu, G., Westbrooks, J. M., Davidson, A. L., & Chen, J. (2005). ATP hydrolysis is required to reset the ATP-binding cassette dimer into the resting-state conformation. *Proceedings of the National Academy of Sciences of the United States of America*, *102*(50), 17969-17974.
39. Zaitseva, J., Jenewein, S., Jumpertz, T., Holland, I. B., & Schmitt, L. (2005). H662 is the

linchpin of ATP hydrolysis in the nucleotide‐binding domain of the ABC transporter HlyB. *The EMBO journal*, *24*(11), 1901-1910.

40. Dawson, R. J., & Locher, K. P. (2006). Structure of a bacterial multidrug ABC transporter. *Nature*, *443*(7108), 180-185.
41. Kitaoka, S., Wada, K., Hasegawa, Y., Minami, Y., Fukuyama, K., & Takahashi, Y. (2006). Crystal structure of Escherichia coli SufC, an ABC-type ATPase component of the SUF iron–sulfur cluster assembly machinery. *FEBS letters*, *580*(1), 137-143.
42. Pinkett, H. W., Lee, A. T., Lum, P., Locher, K. P., & Rees, D. C. (2007). An inward-facing conformation of a putative metal-chelate-type ABC transporter. *Science*, *315*(5810), 373-377.
43. Chang, G. & Roth, C. B. (2001). Structure of MsbA from *E. coli*: a homolog of the multidrug resistance ATP binding cassette (ABC) transporters. *Science 293*, 1793.
44. Doerrler, W. T., Reedy, M. C., & Raetz, C. R. (2001). An *Escherichia coli* mutant defective in lipid export. *Journal of Biological Chemistry*, *276*(15), 11461-11464.
45. Doerrler, W. T., Gibbons, H. S., & Raetz, C. R. (2004). MsbA-dependent translocation of lipids across the inner membrane of *Escherichia coli*. *Journal of Biological Chemistry*, *279*(43), 45102-45109.
46. Zhou, Z., White, K. A., Polissi, A., Georgopoulos, C., & Raetz, C. R. (1998). Function of *Escherichia coli* MsbA, an essential ABC family transporter, in lipid A and phospholipid biosynthesis. *Journal of Biological Chemistry*, *273*(20), 12466-12475.
47. Doerrler, W. T., & Raetz, C. R. (2002). ATPase activity of the MsbA lipid flippase of *Escherichia coli*. *Journal of Biological Chemistry*, *277*(39), 36697-36705.
48. Ward, A., Reyes, C. L., Yu, J., Roth, C. B., & Chang, G. (2007). Flexibility in the ABC transporter MsbA: Alternating access with a twist. *Proceedings of the National Academy of Sciences*, *104*(48), 19005-19010.
49. Eckford, P. D., & Sharom, F. J. (2008). Functional characterization of *Escherichia coli* MsbA interaction with nucleotides and substrates. *Journal of Biological Chemistry*, *283*(19), 12840-12850.
50. Eckford, P. D., & Sharom, F. J. (2010). The reconstituted *Escherichia coli* MsbA protein displays lipid flippase activity. *Biochemical Journal*, *429*(1), 195-203.
51. Siarheyeva, A., & Sharom, F. J. (2009). The ABC transporter MsbA interacts with lipid A and amphipathic drugs at different sites. *Biochemical Journal*, *419*(2), 317-328.
52. Krause, F., & Seelert, H. (2008). Detection and Analysis of Protein‐Protein Interactions of Organellar and Prokaryotic Proteomes by Blue Native and Colorless Native Gel Electrophoresis. *Current Protocols in Protein Science*, 19-18.
53. Westfahl, K. M., Merten, J. A., Buchaklian, A. H., & Klug, C. S. (2008). Functionally Important ATP Binding and Hydrolysis Sites in *Escherichia coli* MsbA. *Biochemistry*, *47*(52), 13878-13886.
54. Schultz, K. M., Merten, J. A., & Klug, C. S. (2011). Characterization of the E506Q and

H537A dysfunctional mutants in the *E. coli* ABC transporter MsbA. *Biochemistry*, *50*(18), 3599-3608.

55. Zou, P., & Mchaourab, H. S. (2009). Mapping daunorubicin-binding sites in the ATP-binding cassette transporter MsbA using site-specific quenching by spin labels. *Journal of Biological Chemistry*, *284*(20), 13904-13913.
56. Poolman, B., Doeven, M. K., Geertsma, E. R., Biemans‐Oldehinkel, E., Konings, W. N., & Rees, D. C. (2005). Functional Analysis of Detergent‐Solubilized and Membrane‐Reconstituted ATP‐Binding Cassette Transporters. *Methods in enzymology*, *400*, 429-459.
57. Kawai, T., Caaveiro, J. M., Abe, R., Katagiri, T., & Tsumoto, K. (2011). Catalytic activity of MsbA reconstituted in nanodisc particles is modulated by remote interactions with the bilayer. *FEBS letters*, *585*(22), 3533-3537.
58. Urbatsch, I. L., Sankaran, B., Weber, J., & Senior, A. E. (1995). P-glycoprotein is stably inhibited by vanadate-induced trapping of nucleotide at a single catalytic site. *Journal of Biological Chemistry*, *270*(33), 19383-19390.
59. Hockney, R. C. (1994). Recent developments in heterologous protein production in *Escherichia coli*. *Trends in biotechnology*, *12*(11), 456-463.
60. Miroux, B., & Walker, J. E. (1996). Over-production of proteins in *Escherichia coli*: mutant hosts that allow synthesis of some membrane proteins and globular proteins at high levels. *Journal of molecular biology*, *260*(3), 289-298.
61. Wagner, S., Klepsch, M. M., Schlegel, S., Appel, A., Draheim, R., Tarry, M., ... & De Gier, J. W. (2008). Tuning *Escherichia coli* for membrane protein overexpression. *Proceedings of the National Academy of Sciences*, *105*(38), 14371-14376.
62. Braun, R. J., Kinkl, N., Beer, M., & Ueffing, M. (2007). Two-dimensional electrophoresis of membrane proteins. *Analytical and bioanalytical chemistry*, *389*(4), 1033-1045.
63. Wittig, I., & Schägger, H. (2005). Advantages and limitations of clear‐native PAGE. *Proteomics*, *5*(17), 4338-4346.
64. Sauna, Z. E., Smith, M. M., Müller, M., & Ambudkar, S. V. (2001). Evidence for the vectorial nature of drug (substrate)-stimulated ATP hydrolysis by human P-glycoprotein. *Journal of Biological Chemistry*, *276*(36), 33301-33304.
65. Segrest, J. P. (1977). Amphipathic helixes and plasma lipoproteins: thermodynamic and geometric considerations. *Chemistry and physics of lipids*, *18*(1), 7-22.
66. Mizrachi, D., Chen, Y., Liu, J., Peng, H. M., Ke, A., Pollack, L., ... & DeLisa, M. P. (2015). Making water-soluble integral membrane proteins in vivo using an amphipathic protein fusion strategy. *Nature communications*, *6*.
67. Sun, H., Molday, R. S., & Nathans, J. (1999). Retinal stimulates ATP hydrolysis by purified and reconstituted ABCR, the photoreceptor-specific ATP-binding cassette transporter responsible for Stargardt disease. *Journal of Biological Chemistry*, *274*(12), 8269-8281.

68. Ketchum, C. J., Schmidt, W. K., Rajendrakumar, G. V., Michaelis, S., & Maloney, P. C. (2001). The yeast a-factor transporter Ste6p, a member of the ABC superfamily, couples ATP hydrolysis to pheromone export. *Journal of Biological Chemistry*, *276*(31), 29007-29011.
69. Gorbulev, S., Abele, R., & Tampé, R. (2001). Allosteric crosstalk between peptide-binding, transport, and ATP hydrolysis of the ABC transporter TAP. *Proceedings of the National Academy of Sciences*, *98*(7), 3732-3737.

Appendices

Appendix A Primers used in the study

Table A.1 Primers used in the study

Primer Name	Sequence 5' to 3'	Product
IPIPE1 forward	ctttaagaaggagatataccatgggtcatcatcatca	MSP
IPIPE1 reverse	ttgtcgttatgcatgccccctgggtattcagcttttag	MSP
VPIPE1 forward	agctgaatacccaggggggcatgcataacgacaaagatct	pET28-His$_7$-MsbA
VPIPE1 reverse	tgatgatgatgatgacccatggtatatctccttcttaaag	pET28-His$_7$-MsbA
IPIPE2 forward	catcatcatcatcatcatcacaaaatcgaagaaggtaaa	MBP
IPIPE2 reverse	agtagtaggaatatcataatccttggtgatacgagtctgcgc	MBP
VPIPE2 forward	gcgcagactcgtatcaccaaggattatgatattcctactact	pET28-His$_7$-MSP-MsbA
VPIPE2 reverse	tttaccttcttcgattttgtgatgatgatgatgatgatg	pET28-His$_7$-MSP-MsbA

IPIPE: Insert-PIPE
VPIPE: Vector-PIPE

The PCR product from IPIPE is inserted into the PCR product from VPIPE.

The products from the first round PCRs, IPIPE1 and VPIPE1 are co-transformed to DH5α competent cells to get the plasmid, pET28-His$_7$-MSP-MsbA
The products from the second round PCRs, IPIPE2 and VPIPE2 are co-transformed to DH5α competent cell to get the final plasmid, pET28-His$_7$-MBP-MSP-MsbA

Appendix B Analysis of MBP-MSP1-MsbA purified in the absence of detergent

B.1 Amylose column purification and native-PAGE analysis

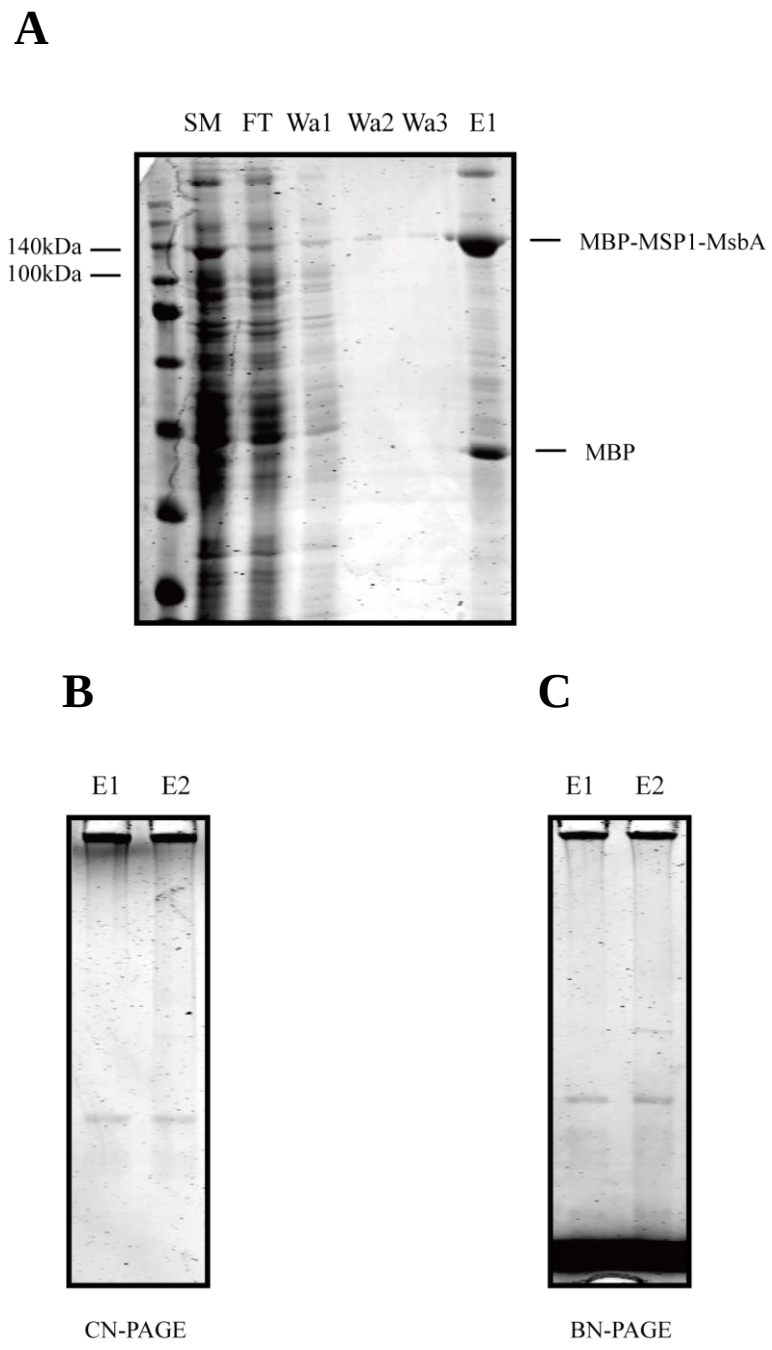

Figure B.1 Amylose column purification and native-PAGE analysis of MBP-MSP1-MsbA purified from soluble fraction in the absence of detergent

A. SDS-PAGE analysis of starting material (SM), flow through (FT), 3 washes (Wa1, 2, 3), and elution fraction from amylose purification of MBP-MSP1-MsbA fusion construct in the absence of detergent. B. Clear-native PAGE analysis of elution fractions of MBP-MSP1-MsbA fusion construct from amylose purification. C. Blue-native PAGE analysis of elution fractions of MBP-MSP1-MsbA fusion construct from amylose purification. The native-PAGE analysis shows the eluted MBP-MSP1-MsbA protein was aggregated.

B.2 Size exclusion chromatography

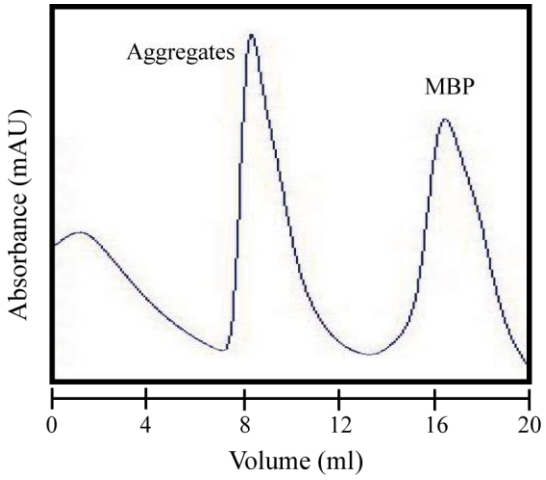

Figure B.2 Size exclusion chromatography of MBP-MSP1-MsbA purified from soluble fraction without detergent

A purified fraction of fusion construct, MBP-MSP1-MsbA from amylose purification of soluble fraction was injected onto a Superdex^{TM} 200 HR 10/300 column equilibrated in buffer C (20 mM Tris-HCl pH 7.9, 200 mM NaCl, 10 % v/v glycerol and 1 mM DTT). It was eluted at the void volume at 8 ml.

Appendix C Analysis of MBP-MSP1-Stop codon construct

C.1 Expression and localization test

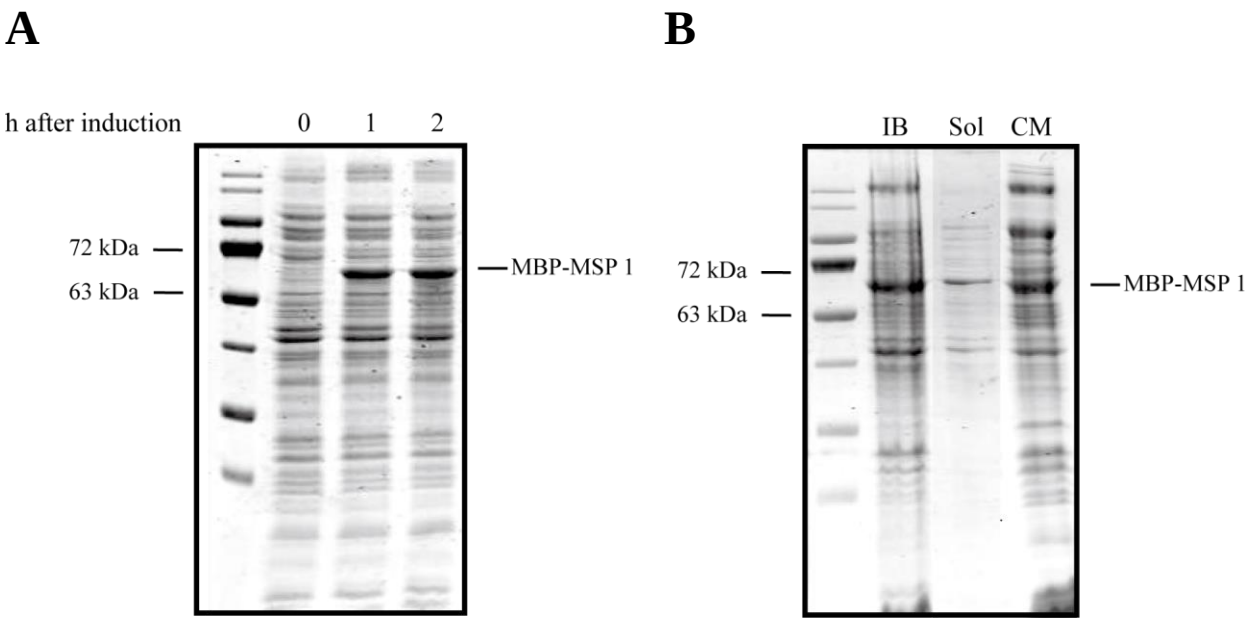

Figure C.1 Expression and localization test of MBP-MSP1 construct

The stop codon insertion construct, MBP-MSP1 was expressed in C43 cell. Its expression was tested after 1 and 2 hours of induction and it was determined whether it was produced as a soluble protein or not on SDS-PAGE. A. Expression of the construct, MBP-MSP1 was analyzed on SDS-PAGE. B. Localization of MBP-MSP1 was analyzed on SDS-PAGE. After cell lysis and fractionation, inclusion body (IB), soluble fraction (Sol), and insoluble membrane fraction (CM) were loaded on SDS-PAGE.

C.2 Purification of MBP-MSP1 by amylose column

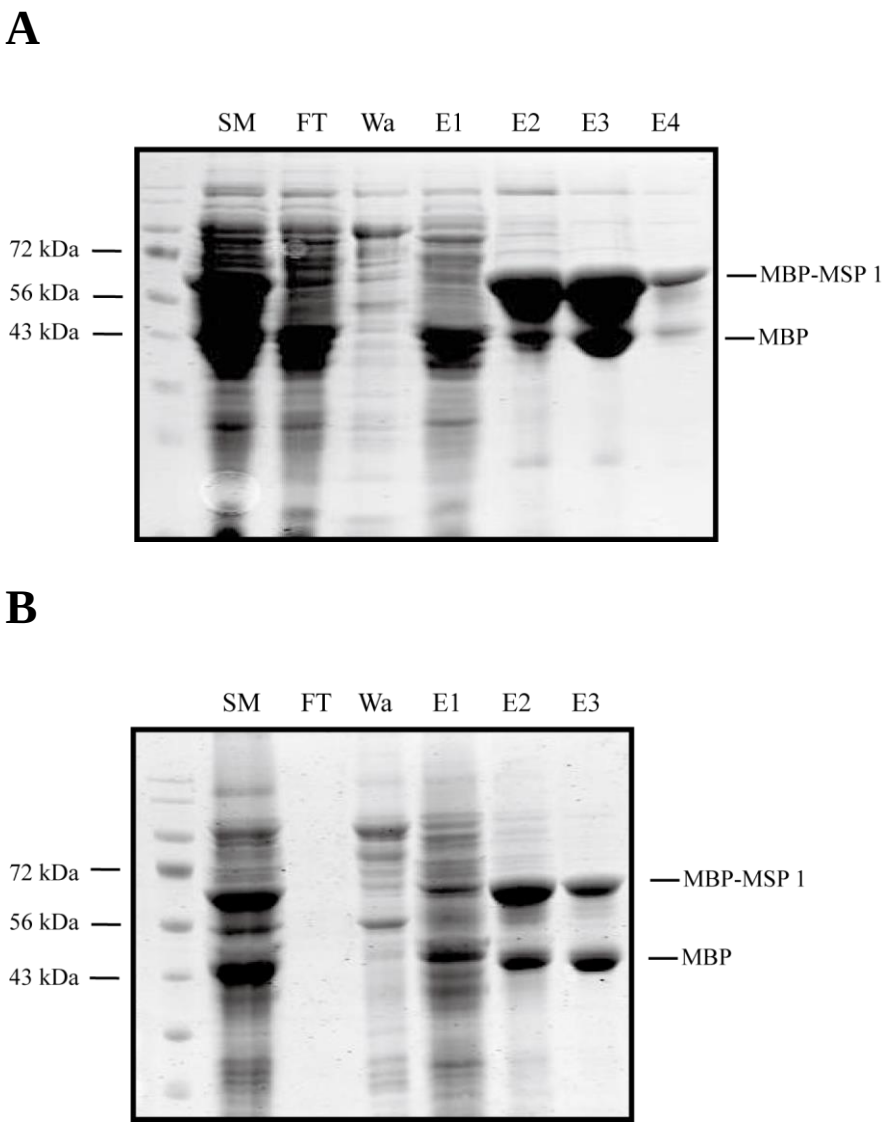

Figure C.2 Purification of MBP-MSP1 by amylose column

The construct, MBP-MSP1 from soluble and insoluble fractions was purified by amylose column. For both purifications, the construct was eluted with 20 mM maltose. A. Purification of MBP-MSP1 from soluble fraction in the absence of Tx-100. Starting material (SM), flow through (FT), wash (Wa), and elution fractions were analyzed by SDS-PAGE. B. Purification of MBP-MSP1 from insoluble fraction in the presence of Tx-100. Starting material (SM), flow through (FT), wash (Wa), and elution fractions were analyzed by SDS-PAGE.